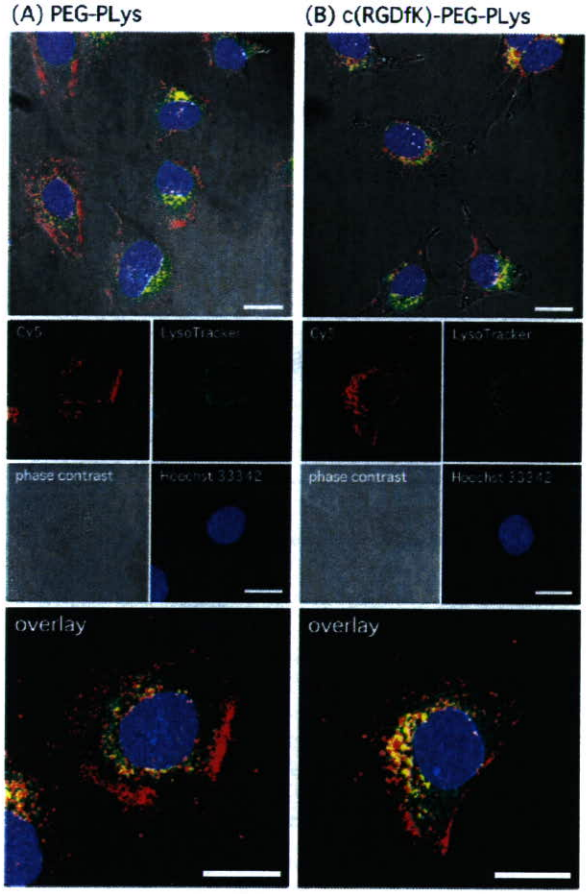

Figure 7. Intracellular distribution of pDNA challenged by the polyplex micelles. PEG−PLys and c(RGDfK)−PEG−PLys micelles loaded with Cy5-labeled pDNA (red) were incubated with HeLa cells for 3 h. The CLSM observation was performed using a 63× objective. The cell nuclei were stained with Hoechst 33342 (blue), and the acidic late endosome and lysosome were stained with LysoTracker Green (green). The scale bar represents 20 μm.

of enhanced uptake and a possible change in the route of intracellular trafficking. These results indicate that the introduction of various peptide ligands including c(RGDfK) peptide into the block copolymers is feasible and could eventually allow the construction of targetable polyplex micelles that are useful for site-specific gene therapy through a systemic route.

ACKNOWLEDGMENT

We thank Ms. K. Date (The University of Tokyo) and Ms. J. Kawakita (The University of Tokyo) for technical assistance. This work was financially supported in part by the Core Research Program for Evolutional Science and Technology (CREST) from Japan Science and Technology Corporation (JST) and the Project on the Materials Development for Innovative NanoDrug Delivery Systems from the Ministry of Education, Culture, Sports, Science and Technology (MEXT), Japan.

LITERATURE CITED

(1) Pedroso de Lima, M. C., Simoes, S., Pires, P., Faneca, H., and Düzgunes, N. (2001) Cationic lipid-DNA complexes in gene delivery: from biophysics to biological applications. *Adv. Drug Delivery Rev. 47*, 277−294.

(2) Merdan, T., Kopecek, J., and Kissel, T. (2002) Prospects for cationic polymers in gene and oligonucleotide therapy against cancer. *Adv. Drug Delivery Rev. 54*, 715−758.

(3) Kakizawa, Y., and Kataoka, K. (2002) Block copolymer micelles for delivery of gene and related compounds. *Adv. Drug Delivery Rev. 54*, 203−222.

(4) Itaka, K., Harada, A., Nakamura, K., Kawaguchi, H., and Kataoka, K. (2002) Evaluation by fluorescence resonance energy transfer of the stability of nonviral gene delivery vectors under physiological conditions. *Biomacromolecules 3*, 841−845.

(5) Harada-Shiba, M., Yamauchi, K., Harada, A., Takamisawa, I., Shimokado, K., and Kataoka, K. (2002) Polyion complex micelles as vectors in gene therapy-pharmacokinetics and in vivo gene transfer. *Gene Ther. 9*, 407−414.

(6) Wakebayashi, D., Nishiyama, N., Yamasaki, Y., Itaka, K., Kanayama, N., Harada, A., Nagasaki, Y., and Kataoka, K. (2004) Lactose-conjugated polyion complex micelles incorporating plasmid DNA as a targetable gene vector system: their preparation and gene transfecting efficiency against cultured HepG2 cells. *J. Controlled Release 95*, 653−664.

(7) Suh, W., Han, S.-O., Yu, L., and Kim, S. W. (2002) An angiogenic, endothelial-cell-targeted polymeric gene carrier. *Mol. Ther. 6*, 664−672.

(8) Ogris, M., Walker, G., Blessing, T., Kircheis, R., Wolschek, M., and Wagner, E. (2003) Tumor-targeted gene therapy: strategies for the preparation of ligand-polyethylene glycol-polyethylenimine/DNA complexes. *J. Controlled Release 91*, 173−181.

(9) Miyata, K., Kakizawa, Y., Nishiyama, N., Yamasaki, Y., Watanabe, T., Kohara, M., and Kataoka, K. (2005) Freeze-dried formulations for in vivo gene delivery of PEGylated polyplex micelles with disulfide crosslinked cores to the liver. *J. Controlled Release 109*, 15−23.

(10) Haubner, R., Gratias, R., Diefenbach, B., Goodman, S. L., Jonczyk, A., and Kessler, H. (1996) Structural and functional aspects of RGD-containing cyclic pentapeptides as highly potent and selective integrin $\alpha_v\beta_3$ antagonist. *J. Am. Chem. Soc. 118*, 7461−7472.

(11) Brooks, P. C., Clark, R. A. F., and Cheresh, D. A. (1994) Requirement of vascular integrin $\alpha_v\beta_3$ for angiogenesis. *Science 264*, 569−571.

(12) Akiyama, Y., Harada, A., Nagasaki, Y., and Kataoka, K. (2000) Synthesis of poly(ethylene glycol)-*block*-poly(ethylenimine) possessing an acetal group at the PEG end. *Macromolecules 33*, 5841−5845.

(13) Harada, A., and Kataoka, K. (1995) Formation of polyion complex micelles in an aqueous milieu from a pair of oppositely charged block copolymers with poly(ethylene glycol) segments. *Macromolecules 28*, 294−299.

(14) Nagasaki, Y., Kutsuna, T., Iijima, M., Kato, M., and Kataoka, K. (1995) Formyl-ended heterobifunctional poly(ethylene oxide): synthesis of poly(ethylene oxide) with a formyl group at one end and a hydroxyl group at the other end. *Bioconjugate Chem. 6*, 231−233.

(15) Poche, D. S., Moore, M. J., and Bowles, J. L. (1999) An unconventional method for purifying *N*-carboxyanhydride derivatives of γ-alkyl-L-glutamates. *Synth. Commun. 29*, 843−854.

(16) Zhang, L., Torgerson, T. R., Liu, X.-Y., Timmons, S., Colosia, A. D., Hawiger, J., and Tam, J. P. (1998) Preparation of functionally active cell-permeable peptides by single-step ligation of two peptide modules. *Proc. Natl. Acad. Sci. U.S.A. 95*, 9184−9189.

(17) LePecq, J.-B., and Paoletti, C. (1967) A fluorescent complex between ethidium bromide and nucleic acids. *J. Mol. Biol. 27*, 87−106.

(18) Itaka, K., Yamauchi, K., Harada, A., Nakamura, K., Kawaguchi, H., and Kataoka, K. (2003) Polyion complex micelles from plasmid DNA and poly(ethylene glycol)-poly(L-lysine) block copolymer as serum-tolerable polyplex system: physicochemical properties of micelles relevant to gene transfection efficiency. *Biomaterials 24*, 4495−4506.

(19) Wakebayashi, D., Nishiyama, N., Itaka, K., Miyata, K., Yamasaki, Y., Harada, A., Koyama, H., Nagasaki, Y., and Kataoka, K. (2004) Polyion complex micelles of pDNA with acetal-poly(ethylene glycol)-poly(2-(dimethylamino)ethyl methacrylate) block copolymer as the gene carrier system: physicochemical properties of micelles relevant to gene transfection efficiency. *Biomacromolecules 5*, 2128−2136.

(20) Pierschbacher, M. D., and Ruoslahti, E. (1984) Cell attachment activity of fibronectin can be duplicated by small synthetic fragments of the molecule. *Nature 309*, 30−33.

(21) Pierschbacher, M. D., and Ruoslahti, E. (1984) Variants of the cell recognition site of fibronectin that retain attachment-promoting activity. *Proc. Natl. Acad. Sci. U.S.A. 81*, 5985−5988.

(22) Dechantsreiter, M. A., Planker, E., Mathä, B., Lohof, E., Hölzemann, G., Jonczyk, A., Goodman, S. L., and Kessler, H. (1999) *N*-Methylated cyclic RGD peptides as highly active and selective $\alpha_v\beta_3$ integrin antagonists. *J. Med. Chem. 42*, 3033−3040.

(23) Allen, T. M. (2002) Ligand-targeted therapeutics in anticancer therapy. *Nat. Rev. 2*, 750−763.

(24) Kim, W. J., Yockman, J. W., Lee, M., Jeong, J. H., Kim, Y.-H., and Kim, S. W. (2005) Soluble *Flt-1* gene delivery using PEI-*g*-PEG-RGD conjugate for anti-angiogenesis. *J. Controlled Release 106*, 224−234.

(25) Kim, W. J., Yockman, J. W., Jeong, J. H., Christensen, L. V., Lee, M., Kim, Y.-H., and Kim, S. W. (2006) Anti-angiogenic inhibition of tumor growth by systemic delivery of PEI-*g*-PEG-RGD/pCMV-sFlt-1 complexes in tumor-bearing mice. *J. Controlled Release 114*, 381−388.

(26) Marinelli, L., Gottschalk, K.-E., Meyer, A., Novellino, E., and Kessler, H. (2004) Human integrin $\alpha_v\beta_5$: homology modeling and ligand binding. *J. Med. Chem. 47*, 4166−4177.

(27) Bretscher, M. S. (1996) Moving membrane up to the front of migrating cells. *Cell 85*, 465−467.

(28) Marnie, R., Simon, B., Alison, W., Peter, S., and Jim, N. (2001) PDGF-regulated rab4-dependent recycling of $\alpha_v\beta_3$ integrin from early endosomes is necessary for cell adhesion and spreading. *Curr. Biol. 11*, 1392−1402.

(29) Suh, J., Wirtz, D., and Hanes, J. (2003) Efficient active transport of gene nanocarriers to the cell nucleus. *Proc. Natl. Acad. Sci. U.S.A. 100*, 3878−3882.

(30) Kulkarni, R. P., Wu, D. D., Davis, M. E., and Fraser, S. E. (2005) Quantitating intracellular transport of polyplexes by spatio-temporal image correlation spectroscopy. *Proc. Natl. Acad. Sci. U.S.A. 102*, 7523−7528.

(31) Rejmna, J., Bragonzi, A., and Conese, M. (2005) Role of clathrin- and caveolae-mediated endocytosis in gene transfer mediated by lipo- and polyplexes. *Mol. Ther. 12*, 468−474.

(32) Gersdorff, K., Sanders, N. N., Vandenbroucke, R., Smedt, S. C., Wagner, E., and Ogris, M. (2006) The internalization route resulting in successful gene expression depends on both cell line and polyethylenimine polyplex type. *Mol. Ther. 14*, 745−753.

BC0700133

GENE DELIVERY

ELSEVIER

Available online at www.sciencedirect.com
ScienceDirect

Journal of Controlled Release 122 (2007) 252–260

journal of controlled release

www.elsevier.com/locate/jconrel

PEG-based block catiomers possessing DNA anchoring and endosomal escaping functions to form polyplex micelles with improved stability and high transfection efficacy

Kanjiro Miyata [a,d], Shigeto Fukushima [b], Nobuhiro Nishiyama [c,d], Yuichi Yamasaki [b,d], Kazunori Kataoka [b,c,d,*]

[a] Department of Bioengineering, School of Engineering, The University of Tokyo, 7-3-1 Hongo, Bunkyo-ku, Tokyo 113-8656, Japan
[b] Department of Materials Engineering, School of Engineering, The University of Tokyo, 7-3-1 Hongo, Bunkyo-ku, Tokyo 113-8656, Japan
[c] Center for Disease Biology and Integrative Medicine, School of Medicine, The University of Tokyo, 7-3-1 Hongo, Bunkyo-ku, Tokyo 113-0033, Japan
[d] Center for NanoBio Integration, The University of Tokyo, 7-3-1 Hongo, Bunkyo-ku, Tokyo 113-8656, Japan

Received 26 May 2007; accepted 19 June 2007
Available online 27 June 2007

Abstract

For the development of polyplex systems showing a high transfection efficacy without a large excess of polycations, a lysine (Lys) unit as a DNA anchoring moiety was introduced into the amino acid sequence in poly(ethylene glycol)-*b*-cationic poly(*N*-substituted asparagine) with a flanking *N*-(2-aminoethyl)-2-aminoethyl group (PEG-*b*-Asp(DET)) resulting in PEG-*b*-P[Lys/Asp(DET)], in which the Asp(DET) unit acts as a buffering moiety inducing endosomal escape with minimal cytotoxicity. PEG-*b*-P[Lys/Asp(DET)]/DNA polyplexes exhibited a narrow size distribution of ~90 nm without secondary aggregates at the stoichiometric N/P 1, suggesting the formation of PEG-shielded polyplex micelles. The introduction of Lys units into the catiomer sequence facilitated cellular uptake and a 100-fold higher level of gene expression with PEG-*b*-P[Lys/Asp(DET)]/DNA polyplex micelles prepared even at a lowered N/P 2, possibly due to the enhanced association power of the anchoring Lys units.

Keywords: Gene delivery; PEG; Polyplex micelle; Block copolymer; Nonviral

1. Introduction

In recent years, enormous efforts have been devoted to the development of polycation-based gene delivery systems (polyplexes) due to their safety for clinical use, simplicity of preparation, and adaptability to large-scale production [1,2]. In particular, poly(ethylene glycol)-modified (PEGylated) polyplexes (polyplex micelles) formed through the electrostatic interaction between plasmid DNA (pDNA) and PEG-*b*-polycation copolymers (PEG-based block catiomers) are promising for *in vivo* gene therapy applications. The unique core-shell architecture of PEG-based block catiomers when combined with pDNA shows particle size data <100 nm under physiological conditions [3]. Indeed, polyplex micelles from PEG-*b*-poly(L-lysine) copolymers showed a high colloidal stability in biological media, excellent biocompatibility, and prolonged circulation periods in the blood stream [4–6]. However, further improvement in the transfection efficacy of these polyplex systems is needed for translation into the clinic.

Previous studies have revealed that a high transfection efficacy was obtained from polycations with a relatively low p*K*a value, such as polyethylenimine (PEI), which is explained by their buffering effect in endosomal compartments, as described by the proton sponge hypothesis [7,8]. In this regard, we have developed PEG-*b*-poly(*N*-substituted asparagine) copolymers having the *N*-(2-aminoethyl)-2-aminoethyl group

* Corresponding author. Department of Materials Engineering, School of Engineering, The University of Tokyo, 7-3-1 Hongo, Bunkyo-ku, Tokyo 113-8656, Japan. Fax: +81 3 5841 7139.
E-mail address: kataoka@bmw.t.u-tokyo.ac.jp (K. Kataoka).

0168-3659/$ - see front matter © 2007 Elsevier B.V. All rights reserved.
doi:10.1016/j.jconrel.2007.06.020

in the side chain (PEG-*b*-PAsp(DET)). Consequently, these polyplex micelles exhibited a remarkably high transfection activity possibly due to the high buffering capacity based on the distinctive two-step protonation behavior of the flanking ethylenediamine moiety [9]. Also, we found that PEG-*b*-PAsp (DET) copolymers showed minimal cytotoxicity, allowing the successful transfection to primary cells [9–12]. However, an excess of PEG-*b*-PAsp(DET) copolymers with high N/P ratios were required for successful polyplex transfection; consequently, we concluded that micelle solutions prepared under such conditions are likely to contain a mixed population of: (i) block catiomers firmly condensing DNA, (ii) block catiomers loosely associated with DNA, and (iii) free or non-DNA condensing block catiomers. Hence, *in vivo* use of such PEG-*b*-PAsp(DET) polyplex micelles, particularly for systemic administration, may be limited, because loosely associated block catiomers easily desorb from the polyplex micelles during blood circulation, leading to the decreased transfection efficacy at the target site. Therefore, the micelle systems showing efficient transfection at lower N/P ratios without such non-associated or loosely associated catiomers should be next developed for *in vivo* gene delivery.

The present study was devoted to improving the transfection efficacy of the PEG-*b*-PAsp(DET)-based polyplex micelles at N/P ratios near unity by enhancing their association power through the introduction of Lys residues into the amino acid sequence of the block catiomer. Note that Lys residues are expected to anchor the associated block catiomers to the polyplex micelles. In this way, a significantly improved efficacy of transfection was achieved with the polyplex micelles with a subtle excess of block catiomers even after preincubation in the medium containing serum. This result seems to be associated with the facilitated cellular internalization of the polyplex micelles with stably incorporated block catiomers showing a high buffering capacity for endosomal escape.

2. Materials and methods

2.1. Materials

α-Methoxy-ω-amino-poly(ethylene glycol) (Mw 12,000) and β-benzyl-L-aspartate *N*-carboxyanhydride (BLA-NCA) were obtained from Nippon Oil and Fats Co., Ltd. (Tokyo, Japan). ε-(Benzyloxycarbonyl)-L-lysine *N*-carboxyanhydride (Lys(Z)-NCA) was synthesized from ε-(benzyloxycarbonyl)-L-lysine (Wako Pure Chemical Industries, Ltd., Osaka, Japan) by the Fuchs–Farthing method using bis(trichloromethyl) carbonate (triphosgene) (Tokyo Kasei Kogyo Co., Ltd., Tokyo, Japan) [13]. Diethylenetriamine (DET), *N,N*-dimethylformamide (DMF), dichloromethane, benzene, and trifluoroacetic acid were purchased from Wako Pure Chemical Industries, Ltd. Hydrogen bromide (HBr) (30% in acetic acid) was purchased from Tokyo Kasei Kogyo Co., Ltd. Branched polyethylenimine (25 kDa) (BPEI) was purchased from Sigma-Aldrich Co. (St. Louis, MO). The pDNA coding for *luciferase* with a CAG promoter (RIKEN, Japan) was amplified in competent DH5α *E. coli* and purified with a QIAGEN HiSpeed Plasmid MaxiKit (Germantown, MD). Luciferase Assay System Kit was purchased from Promega (Madison WI); Label IT Fluorescein Labeling Kit from Mirus Co. (Milwaukee, WI); and Micro BCA™ Protein Assay Reagent Kit from Pierce Co., Inc. (Rockford, IL).

2.2. Synthesis of PEG-b-P[Lys/Asp(DET)]

Block copolymers of PEG and L-lysine(Z)/β-benzyl-L-aspartate copolymer (P[Lys(Z)/BLA]), further referenced as PEG-*b*-P[Lys(Z)/BLA], were synthesized by ring-opening polymerization of a mixture of Lys(Z)-NCA and BLA-NCA initiated by the terminal primary amino group of α-methoxy-ω-amino-PEG (Scheme 1). The typical synthetic procedure is described as follows for the PEG-*b*-P[Lys(Z)/BLA] with 47 units of Lys(Z) and 52 units of BLA. Lys(Z)-NCA (1.29 g) and BLA-NCA (1.25 g) were dissolved in a mixture of DMF and dichloromethane (6.8 mL and 31.7 mL, respectively). This NCA solution was added to the PEG (1.0 g) in dichloromethane (15 mL) in a stream of dry argon and stirred at 35 °C for 48 h for copolymerization. The polymer in the reaction medium was precipitated in a mixture of hexane and ethyl acetate (600 mL and 400 mL, respectively), and purified by filtration. The acetylation of the *N*-terminal amino group of the obtained polymer (1.5 g) was subsequently performed at 35 °C for 1 h using acetic anhydride (500 μL) in a dichloromethane solution (22 mL). The polymer solution was precipitated into a mixture of hexane and ethyl acetate (300 mL and 200 mL, respectively), purified by filtration, and lyophilized from a benzene solution. The resulting copolymers had molecular weight distributions (Mw/Mn) of 1.1 to 1.3 as determined by GPC (data not shown). The degree of polymerization (DP) of the P[Lys(Z)/BLA] segment in the PEG-*b*-P[Lys(Z)/BLA] was determined from the peak intensity ratio of the methylene protons of PEG (OCH_2-CH_2, δ=3.5 ppm) to the aryl protons of the benzyl groups in the

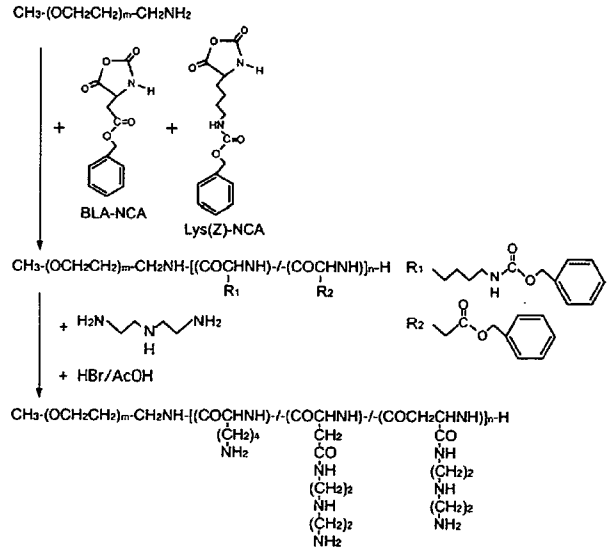

Scheme 1. Synthetic procedure of PEG-*b*-P[Lys/Asp(DET)].

Lys(Z) and BLA units (C_6H_6, δ=7.2–7.3 ppm) in the ^{1}H NMR spectra taken in dimethylsulfoxide at 80 °C. The compositions of the P[Lys(Z)/BLA] segments were determined from the peak intensity ratio of the protons of the β to δ methylene groups ($CH_2CH_2CH_2$, δ=1.2–2.0 ppm) in the side chain of the Lys(Z) units to the protons of the benzyl groups in the Lys(Z) and BLA units in the ^{1}H NMR spectra under the same conditions.

The PEG-*b*-P[Lys(Z)/BLA] copolymers (300 mg) were dissolved in DMF (6 mL), after which DET (2.5 mL; 50 eq to the benzyl group of PBLA) was added to the polymer solution, and stirred for 24 h at 40 °C under a dry argon atmosphere. After 24 h, the mixture was dropped into diethylether (120 mL) with stirring, and then the white precipitate was filtered and re-dissolved in trifluoroacetic acid (4 mL). To deprotect the Z group, HBr (30% in acetic acid) was then added and stirred for 1 h, after which the solution was dropped into diethylether (100 mL) with stirring, and the resulting precipitate was purified by filtered and dried *in vacuo*. The crude product was dissolved in distilled water, dialyzed against 0.01 N HCl and distilled water, and lyophilized to obtain the final product, PEG-*b*-P[Lys/Asp(DET)] as the hydrochloride salt form. The PEG-*b*-P[Lys/Asp(DET)] copolymers with varying ratios of Lys units to Asp (DET) units were obtained by changing the initial feeding ratio of Lys(Z)-NCA to BLA-NCA upon polymerization. The introduction of a DET moiety was confirmed from the peak intensity ratio of the methylene protons of PEG (OCH_2CH_2, δ=3.5 ppm) to the methylene protons of the introduced DET moieties ($CH_2CH_2NHCH_2CH_2$, δ=2.6–3.6 ppm) in the ^{1}H NMR spectra taken in D_2O at 25 °C.

2.3. Preparation of polyplex micelles from PEG-b-P[Lys/Asp (DET)]

The synthesized PEG-*b*-P[Lys/Asp(DET)] copolymer was dissolved in 10 mM Tris–HCl (pH 7.4) buffer at 5 mg/mL. This polymer solution was then mixed with pDNA in 10 mM Tris–HCl (pH 7.4) (50 μg/mL) at varying N/P ratios (residual molar ratio of amino groups in Lys and Asp(DET) units to pDNA phosphate groups), followed by a 24 h incubation at ambient temperature. The final concentration of pDNA in all the samples was adjusted to 33 μg/mL. The complexation of pDNA with the polycations was confirmed by agarose gel retardation analysis and ethidium bromide (EtBr) dye exclusion assay. In the gel retardation analysis, each sample was prepared by the dilution of the micelle solutions to the concentration of 8.3 μg pDNA/mL. 20 μL of each sample (166 ng pDNA) with a loading buffer was then electrophoresed at 100 V for 1 h on a 0.9 wt% agarose gel in 3.3 mM Tris–acetic acid buffer containing 1.7 mM sodium acetate. The migrated pDNA was visualized by soaking the gel in distilled water containing EtBr (0.5 μg/mL). In the EtBr dye exclusion assay, each sample (33 μg pDNA/mL) with varying N/P ratios was adjusted to 10 μg pDNA/mL with 2.5 μg EtBr/mL and 150 mM NaCl by adding 10 mM Tris–HCl (pH 7.4) buffer containing EtBr and NaCl. The solutions were incubated at ambient temperature overnight. The fluorescence intensity of the samples excited at 510 nm was measured at 590 nm and a temperature of 25 °C using a spectrofluorometer (Jasco, FP-777). The relative fluorescence intensity was calculated as follows:

$$F_r = (F_{sample} - F_0)/(F_{100} - F_0)$$

where F_{sample} is the fluorescence intensity of the micelle samples, F_{100} is the free pDNA, and F_0 is the background without pDNA.

2.4. Zeta-potential and dynamic light scattering (DLS) measurements

The zeta-potential of the polyplex micelles was determined from the laser-Doppler electrophoresis using the Zetasizer nanoseries (Malvern Instruments Ltd., UK) at a detection angle of 173° and a temperature of 25 °C. Each sample was prepared by simply mixing the polymer solutions with the pDNA solution at varying N^+/P ratios (33 μg pDNA/mL). The N^+/P ratio was defined as the residual molar ratio of protonated amino groups in PEG-*b*-P[Lys/Asp(DET)] to phosphate groups in DNA. The fraction of protonated amino groups in P[Lys/Asp(DET)] segment was calculated assuming that 100% and 50% of the amino groups in the Lys and Asp(DET) units, respectively, were protonated at pH 7.4 and a temperature of 25 °C based on the potentiometric titration results [9]. The samples were adjusted to 14 μg pDNA/mL by adding 10 mM Tris–HCl (pH 7.4) buffer, and then, injected into folded capillary cells (Malvern Instruments, Ltd.), followed by the measurement. From the obtained electrophoretic mobility, the zeta-potentials of each micelle were calculated by the Smoluchowski equation: $\zeta = 4\pi\eta\upsilon/e$ in which η is the viscosity of the solvent, υ is the electrophoretic mobility, and e is the dielectric constant of the solvent. The results are represented as the average of three experiments.

The sizes of each polyplex micelle were also measured by the DLS using the same apparatus. Micelle samples were prepared by mixing each polymer solution with pDNA solution at varying N^+/P ratios (33 μg pDNA/mL). After an overnight incubation at ambient temperature, the samples were adjusted to 14 μg pDNA/mL by adding 10 mM Tris–HCl (pH 7.4) buffer, and then injected into low volume glass cuvettes, ZEN2112 (Malvern Instruments, Ltd.), followed by the measurement. The data obtained from the rate of decay in the photon correlation function were analyzed by the cumulant method, and the corresponding hydrodynamic diameter of micelles was then calculated by the Stokes–Einstein equation [14].

2.5. Stability of polyplex micelles against counter polyanion exchange reaction

The stability of the polyplex micelle was estimated from the release of pDNA from the micelle caused by the exchange reaction with poly(aspartic acid) (PAsp, DP 66) as a polyanion. Ten mM Tris–HCl buffer (pH 7.4) solutions with varying concentrations of PAsp were added to the micelle solution with the pDNA concentration of 33 μg/mL. After overnight incubation at ambient temperature, each sample solution containing 167 ng of pDNA was electrophoresed through a 0.9 wt% agarose gel with

a running buffer of (3.3 mM Tris–acetic acid (pH 7.4)+1.7 mM sodium acetate+1 mM EDTA2Na). The pDNAs in the gel were visualized by soaking the gel into distilled water containing EtBr (0.5 mg/L).

2.6. Radiolabeling of pDNA for the cellular uptake study of polyplex micelles

pDNA was radioactively labeled with ^{32}P-dCTP using the Nick Translation System (Invitrogen, San Diego, CA). Unincorporated nucleotides were removed using High Pure PCR Product Purification Kit (Roche Laboratories, Nutley, NJ). After the purification, the 2 μg of labeled pDNA was mixed with 400 μg of non-labeled pDNA. The polyplex micelle samples were prepared by mixing the radioactive pDNA solution with each polymer solution (33 μg pDNA/mL). For cellular uptake experiments, Hela cells were seeded on 24-well cultured plates 24 h before the experiments in Dulbecco's modified Eagle medium (DMEM) containing 10% fetal bovine serum (FBS). The cells were incubated with 30 μL of the radioactive micelle solution (1 μg pDNA/well) in 400 μL of DMEM containing 10% FBS. After 24 h incubation, the cells were washed three times with Dulbecco's PBS and lysed with 400 μL of the cell culture Promega lysis buffer. The lysates were mixed with 5 mL of scintillation cocktail, Ultima Gold (PerkinElmer, MA), and then, the radioactivity of the lysate solution was measured by a scintillation counter. The results are presented as a mean and standard error of mean obtained from four samples.

2.7. In vitro transfection

Hela cells were seeded on 24-well culture plates and incubated overnight in 400 μL of DMEM containing 10% FBS. The medium was changed to 400 μL of fresh DMEM containing 10% FBS, and then 30 μL of each micelle solution was applied to each well (1 μg of pDNA/well). In the estimation of the effect of serum incubation on the transfection capacity of the micelle samples, the micelle solutions were preincubated with DMEM containing 10% FBS for 4 h and then added to the wells. After 24 h incubation, the medium was changed to 400 μL of fresh DMEM without micelle samples, followed by an additional 24 h incubation. The cells were washed with 400 μL of Dulbecco's PBS, and lysed by 100 μL of the cell culture Promega lysis buffer. The luciferase activity of the lysates was evaluated from the photoluminescence intensity using Mithras LB 940 (Berthold Technologies). The obtained luciferase activity was normalized with the amount of proteins in the lysates determined by the Micro BCA™ Protein Assay Reagent Kit (Pierce).

Table 1
A series of synthesized block catiomers

Code	Feeding unit radio (Lys: Asp)	DP of poly (amino acid)	Unit number of Lys in poly(amino acid)	% of Lys units
L0/101	0:120	101	0	0
L24/102	25:90	102	24	24
L47/99	50:60	99	47	47
L70/98	75:30	98	70	71
L109/109	120:0	109	109	100

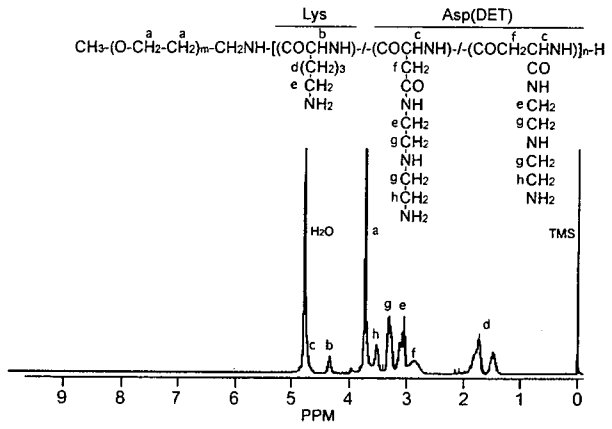

Fig. 1. ^{1}H-NMR spectrum of the PEG-*b*-P[Lys/Asp(DET)] (L47/99) (D_2O; 25 °C; concentration, 10 mg/mL).

2.8. Tolerability of polyplex micelles in serum-containing medium

The tolerability of polyplex micelles in serum-containing medium was estimated from the change in the fluorescence intensity of the fluorescein-labeled pDNA (F-pDNA) contained in the micelles. A pDNA was labeled using a Label IT Fluorescein Labeling Kit. This system promotes the covalent attachment of specific fluorescent molecules to guanine residues in nucleic acids. Each polyplex micelle sample was prepared by simply adding the polymer solution to the F-pDNA solution. After an overnight incubation at ambient temperature under dark conditions, the micelle solutions were mixed with 9 times volume of FBS solution, and then incubated at 37 °C for 4 h. The fluorescence emission of each sample excited at 492 nm was measured at 520 nm and a temperature of 37 °C using a spectrofluorometer (Jasco, FP-777). The obtained fluorescence intensities were expressed as the relative value to the fluorescence intensity of naked F-pDNA.

3. Results and discussion

3.1. Synthesis of PEG-b-P[Lys/Asp(DET)]

Block copolymers of PEG and P[Lys(Z)/BLA] (PEG-*b*-P[Lys(Z)/BLA]) were prepared by the ring-opening copolymerization of Lys(Z)- and BLA-NCAs as shown in Scheme 1. The poly(amino acid) segments with similar DP and varying Lys(Z)/BLA unit ratios were synthesized by changing the feeding ratio of Lys(Z)-NCA to BLA-NCA in the reaction mixture. The DPs and the unit ratios of Lys(Z)/BLA in the obtained copolymers were calculated from the peak intensity ratio in the ^{1}H NMR spectra (data not shown). As summarized in Table 1, five types of copolymers were prepared. The DP of the poly(amino acid) segments in a series of copolymers was confirmed to be approximately 100, regardless of the composition. These copolymers were then subjected to aminolysis reaction with DET, followed

by deprotection of the Z groups. The ^{1}H NMR spectra of the obtained catiomers, as typically seen in Fig. 1, reveal the quantitative aminolysis of BLA units as well as the complete deprotection of Lys(Z) units in the poly(amino acid) segment, because the methylene protons in the DET moiety and the β-methylene protons in the asparagine unit had a 4:1 peak intensity ratio and the peaks of the Z group disappeared in the ^{1}H NMR spectrum. These catiomers were abbreviated as L*x*/*y*, where *x* and *y* represent the unit number of Lys and the total DP of the poly(amino acid) segment, respectively.

3.2. Formation of polyplex micelles from PEG-b-P[Lys/Asp (DET)] catiomers

The polyplex micelles were prepared by simply mixing each catiomer solution with pDNA solution at varying N/P ratios. The complex formation of pDNA was confirmed by the agarose gel electrophoresis of each sample. With an increase in the N/P ratio, the amount of migrating free pDNA decreased, indicating the complex formation of pDNA with the PEG-*b*-P[Lys/Asp (DET)] catiomers (Supplementary Fig. 1). The critical N/P ratio where the migration of pDNA was completely retarded differed depending on the composition of the catiomers; i.e., the micelle of the block catiomers with a lower ratio of Lys units required the higher N/P ratio for the complete retardation of pDNA. To quantitatively evaluate the relationship between the N/P ratio and the condensation behavior of pDNA, the EtBr dye exclusion assay by fluorometry was completed. Fig. 2 (a) shows that the fluorescence intensity of EtBr decreased with an increase in the N/P ratio, and leveled off at a critical N/P ratio for each micelle system. These fluorescence data were then replotted against N^+/P ratio, the molar ratio of protonated amino groups at pH 7.4 in the block catiomers to phosphate groups in pDNA, as seen in Fig. 2 (b). Note that the ratios of the protonated amino groups in the block catiomer were calculated as 100% for Lys units and 50% for Asp(DET) units at pH 7.4, respectively, from the potentiometric titration results of PEG-*b*-PLys and PEG-*b*-PAsp(DET) block catiomers [9,15]. Interestingly, Fig. 2 (b) reveals that the fluorescence intensity of all the micelles leveled off at the N^+/P ratio of approximately 1 regardless of the composition of the catiomers, indicating that the condensation behavior of pDNA might be closely correlated with the ratio of charged groups (N^+/P). Also, this result strongly suggests that the PAsp(DET) segment in the micelles is likely to maintain the same protonation degree ($\alpha = 0.5$ at pH 7.4) as that in the free catiomer without the facilitated protonation by the complexation. As previously reported [9], this limited protonation for the proton sponge potential of the Asp(DET) units in the micelles is assumed to contribute to endosomal escape of PEG-*b*-P[Lys/Asp(DET)] polyplex micelles.

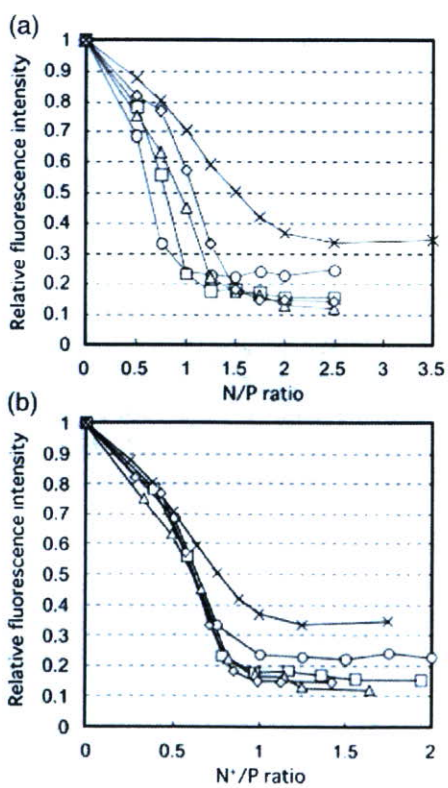

Fig. 2. EtBr dye exclusion assay on a series of polyplex micelles. Micelles included are: ×: L0/101; ◇: L24/102; △: L47/99; □: L70/98; ○: L109/109. (a) Relative fluorescence intensity vs. N/P ratio. (b) Relative fluorescence intensity vs. N^+/P ratio.

Fig. 3 (a) and (b) show the results obtained from DLS and zeta-potential measurements. The cumulant diameters of the polyplex micelles from the PEG-*b*-P[Lys/Asp(DET)]s were determined to be 70–100 nm throughout the range of the examined $N^+/P > 1$. As seen in the Fig. 3 (b) inset, the zeta-potentials of each polyplex micelle appear nearly neutral at an N^+/P 1, indicating the formation of the charge stoichiometric micelle from pDNA and the block catiomers. It should be emphasized that the polyplex micelles from PEG-*b*-P[Lys/Asp(DET)] had a narrowly distributed size of approximately 90 nm without secondary aggregates even at the charge neutralized condition (N^+/P 1) as previously demonstrated for those from PEG-*b*-PLys and PEG-*b*-PAsp(DET) catiomers [9,16]. It should also be noted that all polyplex micelles from the block catiomers had a much lower absolute value in zeta-potentials than polyplexes prepared from PAsp(DET) homopolymer (DP 98) (Fig. 3 (b)), possibly due to the shielding effect of the PEG layer surrounding the polyplex core. Nevertheless, there was a slight increase in the zeta-potentials of the polyplex micelles from neutral to positive values in the region of $N^+/P > 1$. This zeta-potential increase is likely to be ascribed to the loose association of excess catiomers with the polyplex micelles as previously reported for the PEG-poly(2-dimethylamino)ethyl methacrylate) catiomer/pDNA micelle [17]. Interestingly, the tendency of such increasing zeta-potentials with N^+/P ratios varied according to the composition of the block catiomers. The zeta-potential value of the polyplex micelles from PEG-*b*-PLys leveled off at an N^+/P 4 (+10 mV), while that from PEG-*b*-PAsp(DET) seemed to reach a plateau at a higher N^+/P 16 (+10 mV), suggesting that the association profile of the block catiomers with the polyplex micelles varied between PEG-*b*-PLys and PEG-*b*-PAsp(DET) micelles at N^+/P ratios ranging from 1 to 16. Presumably, PEG-*b*-PLys may reach the saturated association with pDNA at the lower

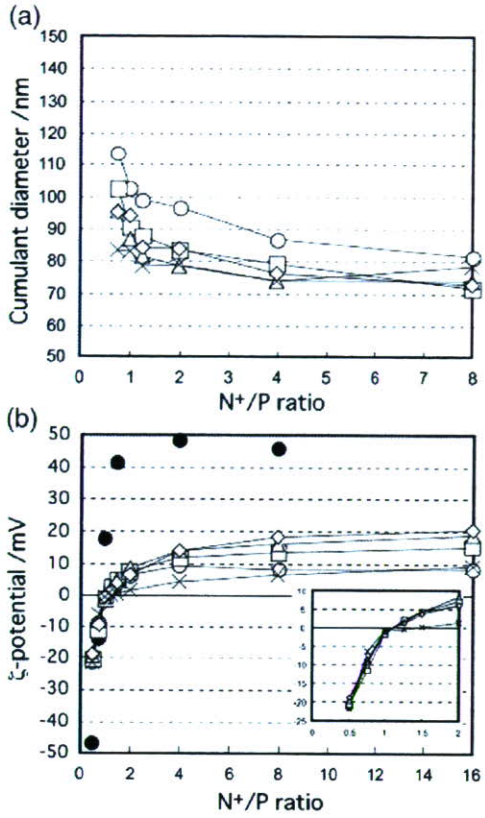

Fig. 3. (a) Size and (b) ζ-potential of a series of polyplex micelles and a PAsp (DET) polyplex. ×: L0/101 micelle, ◇: L24/102 micelle, △: L47/99 micelle, □: L70/98 micelle, ○: L109/109 micelle, ●: PAsp(DET) (DP 98) polyplex.

concentration (lower N^+/P) than PEG-*b*-PAsp(DET) due to the effective anchoring effect of the Lys units. Although PEG-*b*-P[Lys/Asp(DET)] micelles displayed the similar profiles of the zeta-potential to PEG-*b*-PLys micelles at lower N^+/P ratios, the micelles showed further increase in the surface charge in the range of $N^+/P > 4$ without leveling off. This result suggests that the association of PEG-*b*-P[Lys/Asp(DET)] with pDNA may not be saturated even in the range of $N^+/P > 4$, despite introduction of Lys units as a DNA anchoring moiety. This phenomenon may be ascribed to the unique structure of PEG-*b*-P[Lys/Asp(DET)] possessing two types of cationic units with different pDNA affinity. The presence of the Lys units in the block catiomer is likely to facilitate the binding of Asp (DET) units to pDNA, promoting the block catiomer association to the polyplex micelles at N^+/P 2 or lower; however, at high concentrations of the block catiomers (high N^+/P), Lys units may preferentially bind to the polyplex micelles to replace the Asp (DET) units, resulting in the continuous binding of the block catiomers until the Lys units saturate the available binding sites.

3.3. Stability of polyplex micelles

The result of the zeta-potential measurement suggested that the affinity of PAsp(DET) to pDNA seems to be enhanced by the incorporation of Lys units. The complexing stability of the polyplex micelles prepared from PEG-*b*-P[Lys/Asp(DET)] was evaluated directly from the standpoint of the counter polyion exchange reaction. The solutions with varying concentrations of PAsp were added to the solution of the PEG-*b*-PAsp(DET) micelle (N^+/P 2) in different A/P ratios (the molar ratio of carboxyl groups of PAsp to phosphate groups of pDNA). Consequently, the pDNA was released from the PEG-*b*-PAsp (DET) micelles at A/P > 3 due to the counter polyanion exchange of pDNA by PAsp (Fig. 4 (a)). In contrast, the improved stability of the polyplex micelles from PEG-*b*-P[Lys/Asp(DET)] was

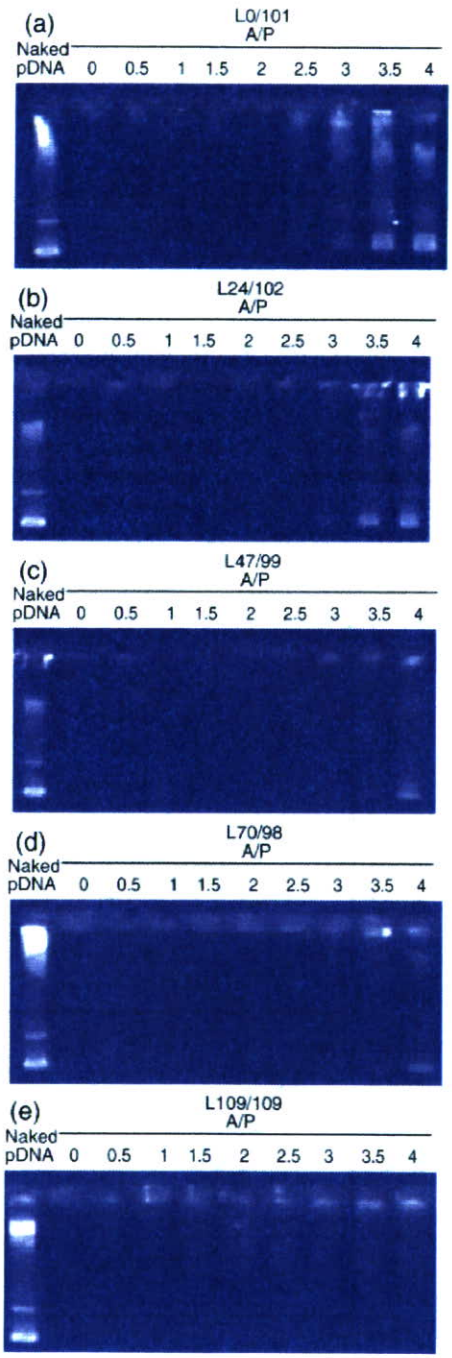

Fig. 4. Electrophoretic evaluation of polyplex micelle (N^+/P 2) tolerability against an exchange reaction with polyaspartic acid (DP 66). Note: A/P stands for the molar ratio of carboxyl groups in polyaspartic acid to phosphate groups in pDNA. Micelle samples prepared at N^+/P 2 were mixed with polyaspartic acid solution and electrophoresed after overnight incubation.

confirmed as shown in Fig. 4 (b)–(d): higher A/P ratios were required for the pDNA release with the increment in the percentage of Lys units in the amino acid sequence of the PEG-*b*-P[Lys/Asp(DET)]. In the case of the micelles from PEG-*b*-PLys, the pDNA release was not observed in the range of the examined A/P ratios (0–4) (Fig. 4 (e)). The similar tendency was also confirmed for the micelles prepared at N^+/P 4 (Supplementary Fig. 2). These results support our hypothesis that a Lys unit has a higher association power with pDNA than the Asp(DET) unit, and consequently, the PEG-*b*-P[Lys/Asp(DET)] micelles acquired the tolerability against the dissociation by polyanions through the anchoring effect of Lys units in the block catiomer.

3.4. Transfection with polyplex micelles from PEG-b-P[Lys/Asp(DET)]

Preliminary experiments on the cellular uptake of complexed pDNA revealed that the pDNA incorporated into PEG-*b*-PAsp (DET) at $N^+/P < 4$ was marginally internalized by cultured cells as is the case with naked pDNA (Supplementary Fig. 3). We speculate that this may contribute to the significantly lower transfection ability of PEG-*b*-PAsp(DET) micelles prepared at low N^+/P ratios. Herein, we hypothesize that the complexing stability promoted by the Lys anchors may facilitate the cellular uptake of polyplex micelles prepared even at low N^+/P ratios. To confirm this hypothesis, we completed a cellular uptake study using ^{32}P-radiolabeled pDNA. Fig. 5 reveals that the cellular uptake of pDNA complexed with block catiomers at an N^+/P ratio of 2 increased by the introduction of the Lys unit into the amino acid sequence. Especially, the polyplex micelles from the PEG-*b*-P[Lys/Asp(DET)] with the percentage of Lys units >47 exhibited more than a 10-fold uptake of pDNA compared to PEG-*b*-PAsp (DET). This result strongly suggests that the increased association power of the polyplex micelles may contribute to their facilitated cellular uptake without a large excess of block catiomers, i.e., at low N^+/P ratios. Interestingly, the cellular uptake of radioactive pDNA was maximized at the L70/98, even through its stability was deemed comparable to that of PEG-*b*-PLys (L109/109), as evidenced from the counter polyanion exchange reaction (Fig. 4

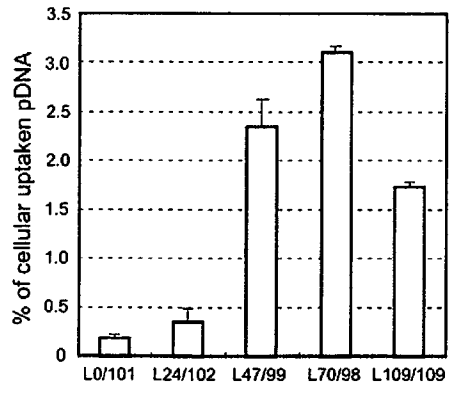

Fig. 5. The uptake of pDNA complexed with block catiomers at N^+/P 2 into Hela cells. ^{32}P-labeled pDNA micelles were incubated with the cells in DMEM containing 10% FBS at 37 °C for 24 h. The amount of internalized pDNA is represented as a percentage for the dosed pDNA (1 μg/well).

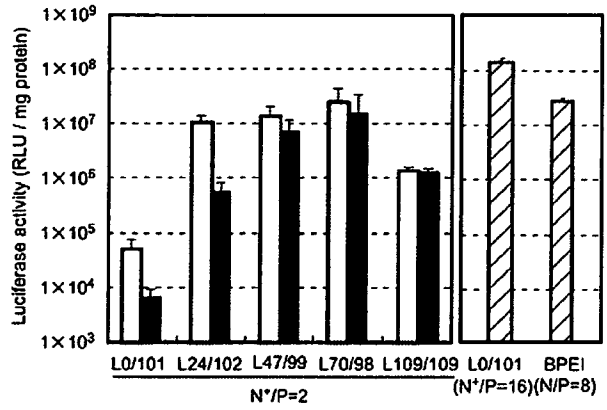

Fig. 6. *In vitro* transfection efficacy of polyplex micelles (N^+/P 2) against Hela cells. Open bars: Transfection efficacy without serum-preincubation. Closed bars: Transfection efficacy after 4 h incubation in the DMEM containing 10% FBS. Hatched bars: Transfection efficacy of the control; L0/101 micelles (N^+/P 16) and BPEI (25 kDa) polyplexes (N/P 8).

(d) and (e)). These data indicate that the increased cellular uptake of PEG-*b*-P[Lys/Asp(DET)] micelles compared to PEG-*b*-PLys micelles was not simply correlated to the enhanced stability. In this regard, a slightly positive zeta-potential of PEG-*b*-P[Lys/Asp (DET)] micelles compared to PEG-*b*-PAsp(DET) and PEG-*b*-PLys micelles is noteworthy, suggesting the surface charge may indeed affect the cellular uptake of the micelles with varying stabilities.

The effect of the introduction of the Lys unit as an anchoring moiety on the transfection ability of the polyplex micelles was then evaluated from the expression of a luciferase gene in the transfected cells. Although the PEG-*b*-PAsp(DET) micelles prepared at the high N^+/P 16 (ca. N/P 32) showed appreciably high transfection efficacy, which was one order of magnitude higher than that of BPEI polyplexes (25 kDa, N/P 8), reduction in the N^+/P ratio resulted in a sharp decline of the transfection ability of the PEG-*b*-PAsp(DET) micelles probably due to the lowered cellular uptake (Fig. 6). In contrast, the transfection efficacy could be maintained to be a high value even in the range of lowered N^+/P ratios by introducing Lys units into the block catiomer (Supplementary Fig. 4). Eventually, the PEG-*b*-P[Lys/Asp(DET)] micelles revealed an appreciably improved transfection efficacy at N^+/P 2 compared to the polyplex micelles of PEG-*b*-PLys and PEG-*b*-PAsp(DET) (Fig. 6, open bars). These results suggest that PEG-*b*-P[Lys/Asp(DET)] micelles may provide high stability and promote endosomal escape, presumably due to the synergistic effect of Lys and Asp(DET) units. The improved stability through the anchoring effect of Lys units was also confirmed from the transfection results after the preincubation of micelles in the serum-containing medium (Fig. 6, closed bars). The micelles from PEG-*b*-P[Lys/Asp(DET)], with the higher percentage of Lys units (L47/99 and L70/98), maintained the initial transfection capacity even after the serum-preincubation, whereas transfection efficacies of PEG-*b*-PAsp(DET) and L24/102 micelles, with a low percentage of Lys residues, were significantly impaired by serum-preincubation. These results strongly suggest that the associated block catiomers in the micelles from L47/99, L70/98, and L109/109 might be tolerable

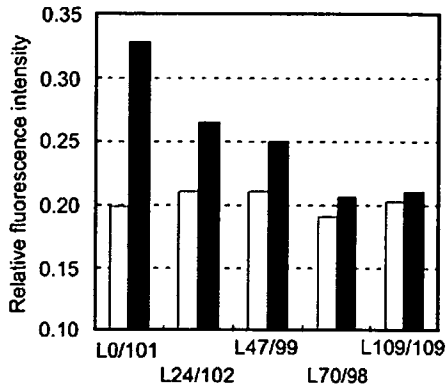

Fig. 7. Tolerability of polyplex micelles against serum incubation evaluated from the fluorescence recovery of the entrapped fluorescein-labeled pDNA due to serum-induced decondensation. Open bars: Fluorescence intensity in 10 mM Tris–HCl (pH 7.4) buffer solution without FBS. Closed bars: Fluorescence intensity after 4 h incubation in the medium containing 90% FBS.

in the transfection medium containing serum due to the strong anchoring of Lys units. This added strength of the Lys anchors is further supported by the sustained fluorescence quenching of fluorescein-labeled pDNA in micelles incubated in 90% FBS for 4 h as seen in Fig. 7. Apparently, fluorescence recovery due to the serum-inducing decondensation of pDNA was progressively inhibited with the increment in the percentage of Lys units in the PEG-*b*-P[Lys/Asp(DET)].

Although the transfection efficacy (Fig. 6) seems to be roughly correlated with the cellular uptake of the micelles (Fig. 5), careful examination reveals the tendency that the PEG-*b*-P[Lys/Asp(DET)] micelles with the lower percentage of Lys units, L24/102, achieved comparable transfection to those with the higher percentage of Lys units, 47/L98 and L70/98, even though the efficacy of pDNA uptake was fairly limited. This tendency becomes more apparent by normalizing the luciferase activity with pDNA uptake (Supplementary Fig. 5). This apparent increase in the transfection efficacy may be explained by the timely release of the loosely associated block catiomers from the micelles in the endosomal compartment to exert a high buffering capacity [9] and their possible interaction with the endosomal membrane component, facilitating the endosomal escape of the complexed pDNA, followed by a smooth release of pDNA directing efficient transcription. The loosely associated nature of L24/102 in the micelle may be supported from a decreased transfection efficacy after serum-preincubation as shown in Fig. 6.

4. Conclusion

Polyplex micelles from PEG-*b*-PAsp(DET) revealed a high transfection efficacy to various cell types including primary cells [9–12] presumably due to a low cytotoxicity and a strong pH-buffering capacity. Nevertheless, the weak association power of PAsp(DET) with DNA may be problematic for *in vivo* systemic administration, where the tolerability of polyplexes in proteinaceous media should be a crucial factor. Alternatively, a polylysine has an appreciably high affinity to DNA, however, the transfection efficacy of polylysine polyplexes remains low, possibly due to poor endosomal escaping functions and an impaired release of pDNA from the polyplex with an over-stabilized nature. In this novel study, we sought to alter these discrepancies by placing both Asp(DET) as a buffering unit with low cytotoxicity and Lys as a strong anchoring moiety to DNA in a single polymer strand resulting in PEG-*b*-P[Lys/Asp(DET)]. Polyplexes prepared from pDNA and PEG-*b*-P[Lys/Asp(DET)] have a micellar structure with a PEG palisade, exhibiting a remarkably improved stability compared to PEG-*b*-PAsp(DET)/pDNA polyplex micelles. PEG-*b*-P[Lys/Asp(DET)] polyplex micelles were further revealed to promote cellular internalization, leading to enhanced transfection efficacy even with a subtle excess of block catiomers. This enhanced transfection efficacy could be explained by the synergistic effect of Lys as an anchoring unit and Asp(DET) as a lower toxic endosomal escaping unit. This approach of placing cationic units with discriminating functions, e.g., DNA anchoring and endosomal escaping functions, into a single block catiomer strand is highly promising for future construct designs for effective *in vivo* systemic applications.

Acknowledgement

This work was financially supported by Research Fellowships of the Japan Society for the Promotion of Science for Young Scientists (JSPS), the Mitsubishi Chemical Corporation Fund, and the Core Research Program for Evolutional Science and Technology (CREST) from the Japan Science and Technology Corporation (JST). The authors express their appreciation to Dr H. Hamada (RIKEN, Japan) for providing the plasmid DNA.

Appendix A. Supplementary data

Supplementary data associated with this article can be found, in the online version, at doi:10.1016/j.jconrel.2007.06.020.

References

[1] D.W. Pack, A.S. Hoffman, S. Pun, P.S. Stayton, Design and development of polymers for gene delivery, Nat. Rev. Drug Discov. 4 (2005) 581–593.
[2] E. Mastrobattista, M.A.E.M. van der Aa, W.E. Hennink, D.J.A. Crommelin, Artificial viruses: a nanotechnological approach to gene delivery, Nat. Rev. Drug Discov. 5 (2006) 115–121.
[3] K. Kakizawa, K. Kataoka, Block copolymer micelles for delivery of gene and related compounds, Adv. Drug Deliv. Rev. 54 (2002) 203–222.
[4] K. Itaka, A. Harada, K. Nakamura, H. Kawaguchi, K. Kataoka, Evaluation by fluorescence resonance energy transfer of the stability of nonviral gene delivery vectors under physiological conditions, Biomacromolecules 3 (2002) 841–845.
[5] M. Harada-Shiba, K. Yamauchi, A. Harada, I. Takamisawa, K. Shimokado, K. Kataoka, Polyion complex micelles as a vector in gene therapy-pharmacokinetics and in vivo gene transfer, Gene Ther. 9 (2002) 407–414.
[6] K. Miyata, Y. Kakizawa, N. Nishiyama, Y. Yamasaki, T. Watanabe, M. Kohara, K. Kataoka, Freeze-dried formulations for in vivo gene delivery of PEGylated polyplex micelles with disulfide crosslinked cores to the liver, J. Control. Release 109 (2005) 15–23.
[7] O. Boussif, F. Lezoualc'h, M.A. Zanta, M.D. Mergny, D. Scherman, B. Demeneix, J.-P. Behr, A versatile vector for gene and oligonucleotide transfer into cells in culture and in vivo: Polyethylenimine, Proc. Natl. Acad. Sci. U. S. A. 92 (1995) 7297–7301.

[8] M. Neu, D. Fischer, T. Kissel, Recent advances in rational gene transfer vector design based on poly(ethylene imine) and its derivatives, J. Gene Med. 7 (2005) 992–1009.

[9] N. Kanayama, S. Fukushima, N. Nishiyama, K. Itaka, W.-D. Jang, K. Miyata, Y. Yamasaki, K. Kataoka, PEG-based biocompatible block catiomer with high-buffering capacity for the construction of polyplex micelles showing efficient gene transfer toward primary cells, ChemMedChem 1 (2006) 439–444.

[10] D. Akagi, M. Oba, H. Koyama, N. Nishiyama, S. Fukushima, T. Miyata, H. Nagawa, K. Kataoka, Biocompatible micellar nanovectors achieve efficient gene transfer to vascular lesions without cytotoxicity and thrombus formation, Gene Ther. 14 (2007) 1029–1038.

[11] M. Han, Y. Bae, N. Nishiyama, K. Miyata, M. Oba, K. Kataoka, Transfection study using multicellular tumor spheroids for screening non-viral polymeric gene vectors with low cytotoxicity and high transfection efficiencies, J. Control. Release, in press.

[12] K. Itaka, S. Ohba, K. Miyata, H. Kawaguchi, K. Nakamura, T. Takato, U. Chung, K. Kataoka, Bone regeneration by regulated in vivo gene transfer using biocompatible polyplex nanomicelles, Mol. Ther., in press.

[13] W.H. Daly, D. Poche, The preparation of *N*-carboxyanhydrides of alpha-amino-acids using bis(trichloromethyl)carbonate, Tetrahedron Lett. 29 (1988) 5859–5862.

[14] A. Harada, K. Kataoka, Formation of polyion complex micelles in an aqueous milieu from a pair of oppositely-charged block-copolymers with poly(ethylene glycol) segments, Macromolecules 28 (1995) 5294–5299.

[15] A. Harada, S. Cammas, K. Kataoka, Stabilized α-helix structure of poly (L-lysine)-block-poly(ethylene glycol) in aqueous medium through supramolecular assembly, Macromolecules 29 (1996) 6183–6188.

[16] K. Itaka, K. Yamauchi, A. Harada, K. Nakamura, H. Kawaguchi, K. Kataoka, Polyion complex micelles from plasmid DNA and poly(ethylene glycol)-poly(L-lysine) block copolymer as serum-tolerable polyplex system: physicochemical properties of micelles relevant to gene transfection efficiency, Biomaterials 24 (2003) 4495–4506.

[17] D. Wakebayashi, N. Nishiyama, K. Itaka, K. Miyata, Y. Yamasaki, A. Harada, H. Koyama, Y. Nagasaki, K. Kataoka, Polyion complex micelles of pDNA with acetal-poly(ethylene glycol)-poly(2-(dimethylamino(ethyl methacrylate) block copolymer as the gene carrier system: Physicochemical properties of micelles relevant to gene transfection efficacy, Biomacromolecules 5 (2004) 2128–2136.

CHEMMEDCHEM

DOI: 10.1002/cmdc.200700076

Enhanced Growth Inhibition of Hepatic Multicellular Tumor Spheroids by Lactosylated Poly(ethylene glycol)-siRNA Conjugate Formulated in PEGylated Polyplexes

Motoi Oishi,[a] Yukio Nagasaki,*[a, c] Nobuhiro Nishiyama,[d] Keiji Itaka,[d] Motoki Takagi,[e] Akira Shimamoto,[e] Yasuhiro Furuichi,[e] and Kazunori Kataoka*[b, d]

PEGylated polyplexes (lac-PEGylated polyplexes) composed of poly(L-lysine) and lactosylated poly(ethylene glycol)-small interfering RNA conjugate, which inhibits the RecQL1 gene product, were revealed to show an appreciable growth inhibition of multicellular HuH-7 spheroids (human hepatocarcinoma cell lines) for up to 21 days (IC_{50}=6 nM); this system used as an in vitro three-dimensional (3D) model mimicking the in vivo biology of tumors. The PEGylated polyplexes thus prepared had a size of approximately 110 nm with clustered lactose moieties on their periphery as targeting ligands for the asialoglycoprotein-receptor-expressing HuH-7 cells. In contrast, OligofectAMINE/siRNA (cationic lipoplex) was observed to have almost no growth-inhibitory effect against HuH-7 spheroids, even though the lipoplex showed a stronger growth-inhibitory effect than the lac-PEGylated polyplexes on conventional monolayer-cultured HuH-7 cells. The FITC-tagged conjugate in the lac-PEGylated polyplexes showed smooth penetration into the HuH-7 spheroids compared with that in the lipoplexes, as observed by confocal fluorescence-scanning microscopy. This indicates that the small size of approximately 100 nm and the reduced nonspecific interaction due to the nonionic and hydrophilic lactosylated PEG layer contributes to the smooth penetration of the PEGylated polyplexes into the spheroid interior, eventually facilitating their uptake into the cells composing the spheroids. Cellular apoptosis indicating programmed cell death was also observed in the HuH-7 spheroids treated with the PEGylated polyplexes, revealing that the observed growth inhibition was indeed induced by the RNAi of the RecQL1 siRNA. These data suggest that the smart PEGylated polyplexes can indeed penetrate into the multiple cell layers of 3D tumor masses in vivo, exerting therapeutic effects through the RNAi.

Introduction

The targeted delivery of small interfering RNAs (siRNAs)[1] is one of the major challenges in the field of cancer therapy through RNA interference (RNAi),[2] because siRNAs often tend to show low stability against enzymatic degradation, low permeability across the cell membrane, and preferential liver and renal clearance.[3] Therefore, the therapeutic value of siRNAs under in vivo conditions is largely dependent on the development of effective carrier systems which achieve modulated disposition in the body intravenously and accumulation in tumor tissues by enhanced permeability and retention (EPR) effect.[4] A promising strategy in this regard is the combination of PEGylation and carrier, namely a "smart" siRNA carrier (PEGylated polyplex) formulated through the supramolecular assembly (electrostatic interactions) of poly(L-lysine) (PLL) and lactosylated poly(ethylene glycol)-siRNA conjugate (Lac-PEG-siRNA) (Figure 1).[5] These smart PEGylated polyplexes, which have a size of approximately 100 nm, showed the high biocompatibility and enzymatic tolerability due to their segregated polyion complex core surrounded by a palisade of flexible and hydrophilic PEG layers. In particular, these smart PEGylated polyplexes with clustered lactose moieties on their periphery were successfully transported into the monolayer-cultured hepatic tumor cells by mediation of the asialoglycoprotein (ASGP) re-

[a] *Prof. Dr. M. Oishi, Prof. Dr. Y. Nagasaki*
Tsukuba Research Center for Interdisciplinary Materials Science (TIMS), University of Tsukuba, 1-1-1 Ten-noudai, Tsukuba, Ibaraki 305-8573 (Japan)
Fax: (+81) 29-853-5749
E-mail: nagasaki@nagalabo.jp

[b] *Prof. Dr. K. Kataoka*
Division of Clinical Biotechnology Center for Disease Biology and Integrative Medicine, Graduate School of Medicine, The University of Tokyo, 7-3-1 Hongo, Bunkyo-ku, Tokyo 113-0033 (Japan)

[c] *Prof. Dr. Y. Nagasaki*
Master's School of Medical Sciences, Graduate School of Comprehensive Human Sciences, University of Tsukuba, 1-1-1 Ten-noudai, Tsukuba, Ibaraki 305-8573, (Japan)

[d] *Prof. Dr. N. Nishiyama, Prof. Dr. K. Itaka, Prof. Dr. K. Kataoka*
Department of Materials Engineering, Graduate School of Engineering, The University of Tokyo, 7-3-1 Hongo, Bunkyo-ku, Tokyo 113-8656 (Japan)
Fax: (+81) 3-5841-7139
E-mail: kataoka@bmw.t.u-tokyo.ac.jp

[e] *Dr. M. Takagi, Dr. A. Shimamoto, Dr. Y. Furuichi*
GeneCare Research Institute Co., Ltd., 200 Kajiwara, Kamakura, Kanagawa 247-0063 (Japan)

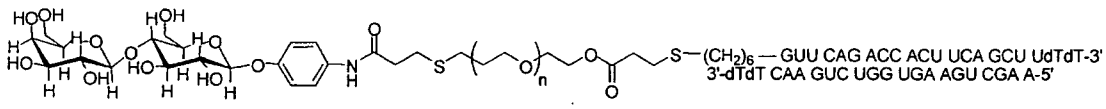

Figure 1. Chemical structure of the Lac-PEG-siRNA conjugate.

ceptor, inducing significant gene silencing of firefly luciferase (reporter gene) expression in monolayer-cultured HuH-7 cells at an extremely low siRNA concentration ($IC_{50} = 1.3$ nM). Therefore, the combination of this smart PEGylated polyplex system and a proper therapeutic siRNA is a promising approach to the creation of a systemic siRNA delivery system for the cancer therapy.

In this regard, siRNA-targeting DNA helicases are of particular interest. DNA helicases have recently been recognized to play important roles in DNA replication, recombination, repair, and transcription. Among many kinds of DNA helicases in living cells, the RecQ helicase family has been shown to have unique properties which are apparently involved in maintaining genomic stability. In humans, the RecQ helicase family has five members: RecQL1, BLM, WRN, RTS, and RecQL5.[6] BLM, WRN, and RTS are causative genes of Bloom syndrome, Werner syndrome, and a subset of Rothmund-Thomson syndrome, respectively, all of which are known to be recessive genetic disorders. Although RecQL1 is not yet known to have a relationship with any human disease, recent findings suggest that it is involved in the maintenance of the human genome.[7] LeRoy et al. have reported that RecQL1 helicase has Holliday junction branch migration activity, and the down-regulation of RecQL1 mRNA by RNAi resulted in an increase in sister chromatid exchange in human cells,[8] suggesting that RecQL1 helicase maintains the human genome by suppressing chromosomal recombination in the S phase. In addition, the RecQL1 protein was up-regulated by mitogenic stimulation or viral transformation in human B-lymphocytes,[9] suggesting that RecQL1 helicase is involved in genomic stabilization in growing cells such as cancer cells. Accordingly, RecQL1 helicase might be a good molecular target in cancer therapy.[10]

We would like to report herein, the significant and prolonged growth inhibition of hepatic multicellular tumor spheroids (MCTSs) by smart PEGylated polyplexes composed of PLL and Lac-PEG-siRNA conjugate bearing a RecQL1-siRNA segment. Note that MCTSs provide an in vivo tumor microenvironment characterized by high cell density, elevated interstitial pressure, hypoxia, and the existence of cell-cell contacts and a tumor extracellular matrix (ECM).[11] Apparently, these environmental factors play key roles in the diffusion, penetration, and growth-inhibitory effects of the siRNA-carriers in solid tumors in vivo. Therefore, using MCTSs, the efficacy of the siRNA delivery systems, including PEGylated polyplexes and lipoplexes, can be simply evaluated from the direct observation of the MCTS size; this method reflects the environmental factors characteristic of tumors and the direct gene silencing ability of the siRNA-carriers.

Results and Discussion

Design of the smart PEGylated polyplexes

Our strategy of formulating PEGylated polyplexes is based on the novel conjugation of siRNA with lactosylated PEG (Lac-PEG-siRNA), followed by complexation with poly(L-lysine) (PLL). The PEG-siRNA conjugates were synthesized according to our previously reported method;[5] the Michael addition of α-lactosyl-ω-acryl-PEG toward the 5'-thiol modified sense RNA to obtain Lac-PEG-single stranded RNA conjugate, followed by annealing with antisense RNA to prepare the Lac-PEG-siRNA conjugate through hybridization. A nonlactosylated conjugate, Ace-PEG-siRNA, was also prepared from the α-acetal-ω-acryl-PEG. The lactosyl-(lac-PEGylated polyplex) and nonlactosyl-(ace-PEGylated polyplex) PEGylated polyplexes were then prepared at an N/P ratio of 1 (=[amino group in polycation]/[phosphate group in siRNA segment]) by mixing the siRNA-PEG conjugates and PLL (degree of polymerization (DP) = 40, 100, or 460). The diameter of the PEGylated polyplex was determined to be approximately 110 nm by TEM.[5]

Growth inhibition of monolayer-cultured tumor cells by the PEGylated polyplexes

The elevation of RecQL1 expression has been positively correlated with various cancer cells, and the depletion of RecQL1 by siRNA complementary to RecQL1 mRNA dramatically inhibited cell proliferation and induced apoptosis in vitro and in vivo.[10] In contrast, the inhibition of the RecQL1 gene product in normal cells by RecQL1 siRNA induces no effect on cell proliferation, suggesting that RecQL1 siRNA is a potential therapeutic tool specific to the molecular targeting of cancer cells. To characterize the growth-inhibitory effect of the PEGylated polyplex system containing RecQL1 siRNA, an MTT assay was done using monolayer-cultured HuH-7 cells (human hepatoma cell) possessing asialoglycoprotein (ASGP) receptors, which recognize and internalize compounds bearing terminal lactose moieties.[12] As seen in Figure 2, almost no growth inhibition was observed for siRNA alone and conjugate alone even at a siRNA concentration of 150 nM in the presence of 10% fetal bovine serum (FBS). On the contrary, lac-PEGylated polyplex with PLL (DP = 100) showed 20% growth inhibition ($P^* < 0.05$) at 150 nM conjugate concentration. These results suggest that the lack of any growth-inhibitory effect on HuH-7 cells for free siRNA and free Lac-PEG-siRNA conjugate may be ascribed to the enzymatic degradation of the siRNA in the medium and to the impaired diffusivity of the negatively charged and hydrophilic free siRNA and Lac-PEG-siRNA conjugate through the negatively charged cell membrane. Significant growth inhibition was observed for the siRNA formulated with commercially

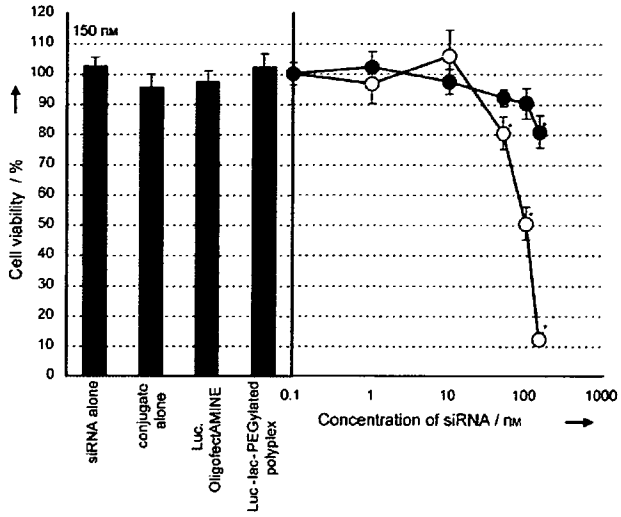

Figure 2. Growth inhibitory effect of the lac-PEGylated polyplexes (closed circles) and lipoplexes (open circles) from RecQL1 siRNA on monolayer-cultured HuH-7 cells. The cell viability was determined by means of an MTT assay after 96 h of incubation. The indicated concentrations of siRNA and conjugate are the final ones in the total transfection volume (250 μL). The plotted data are averages of triplicate experiments ±SD. The data points marked with asterisks are statistically significant compared with the mock data (buffer-treated cells) ($P^* < 0.05$).

available cationic lipid reagents, such as OligofectAMINE (lipoplex) (87% inhibition, $P^* < 0.05$). The lipoplex, which is cationic in character, may strongly interact with the negatively charged cell membrane leading to an appreciable increase in cellular uptake. It should be noticed that the lac-PEGylated polyplex and lipoplex, including luciferase-siRNA as a nontargeted sequence, induced no growth inhibition, strongly suggesting that the observed inhibitory effect against monolayer-cultured HuH-7 cells indeed occurred in a sequence-specific manner through RNAi based on the RecQL1-siRNA.

Growth inhibition of multicellular tumor spheroids (MCTS) by the PEGylated polyplexes

Although the efficacy of the siRNA formulated in the carrier systems in vitro has been generally evaluated by means of monolayer-cultured tumor cells, in vivo results to date have not always been in line with in vitro ones even if the carriers accumulated considerably in the tumor tissues because of the EPR effect. One plausible reason for this discrepancy may be that the monolayer assay only reflects the acute efficacy of the first several days, possibility overlooking the delayed or sustained siRNA action appearing at later stages. Furthermore, the diffusivity of the carriers into the 3D tumor tissue may be crucial in determining the in vivo efficacy, because hypoxic cells that are distant from blood vessels are relatively resistant to chemotherapy, causing the regrowth of the tumor; that is, there are tumor stem cells in the hypoxic regions of some tumors.[13] Therefore, alternatives to in vivo studies (animal experimentations), that is, appropriate in vitro models of in vivo solid tumors, are required to evaluate the prolonged efficacy of siRNA delivery systems, and to properly determine the diffusivity of siRNA-carriers into 3D tumor masses. Worth noting in this regard is the MCTS, which can be maintained in culture medium for many weeks with the physiological characteristics (microenvironment conditions) of in vivo 3D tumor tissues, such as high cell density, elevated interstitial pressure, hypoxia, the existence of cell-cell contacts, and ECM.[11] Indeed, the efficacy of gene delivery by cationic polyplexes and lipoplexes is limited because of their poor penetration ability into MCTSs.[14] Thus, MCTSs were used in this study as 3D in vitro tumor models for screening the growth-inhibitory effect of the siRNAs and their penetration ability into the spheroid interior.

RecQL1 siRNA-mediated growth inhibition of HuH-7 spheroids was assessed under the condition of prolonged culturing (up to 21 days). An HuH-7 spheroid with approximately 100 μm (75–100 μm) in diameter was initially used as the in vitro tumor model, because the maximum distance between the capillary blood vessels within avascular solid tumors is believed to be 200 μm or less.[15] As seen in Figure 3, no growth-inhibitory effect was observed for the siRNA alone or the Lac-PEG-siRNA conjugate alone, even at siRNA concentrations as high as 100 nM. These findings are consistent with the results obtained from the MTT assay using monolayer-cultured HuH-7 cells (Figure 2). In contrast, both the ace-PEGylated and lac-PEGylated polyplexes revealed a significant growth-inhibitory

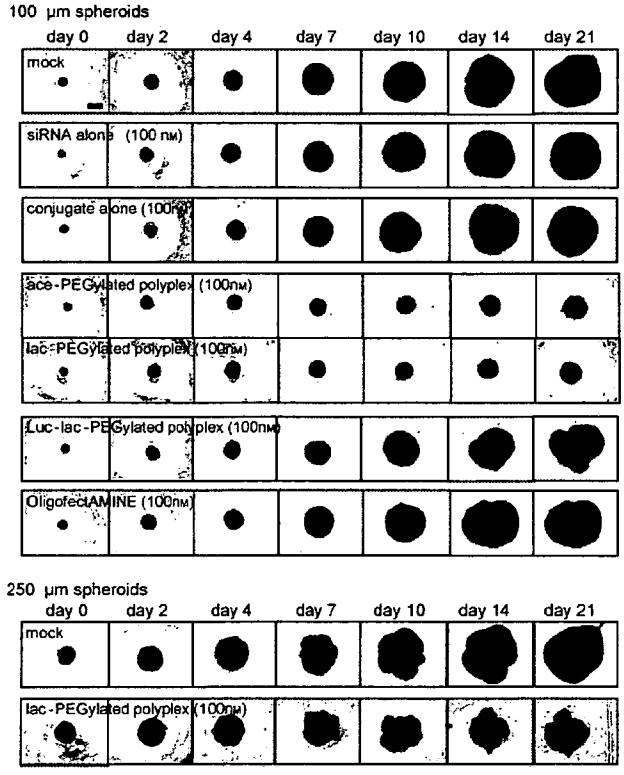

Figure 3. Phase-contrast images of the HuH-7 spheroids with an initial diameter of 100 μm and 250 μm (bar = 100 μm) treated with siRNA alone, Lac-PEG-siRNA conjugate alone, ace-PEGylated polyplex, lac-PEGylated polyplex, Luc-lac-PEGylated polyplex, and OligofectAMINE at concentrations of 100 nM.

effect in a dose-dependent manner (Figure 4a and b). In particular, the lac-PEGylated polyplexes exerted far more effective growth inhibition than the ace-PEGylated polyplexes at a conjugate concentration of as low as 10 nM; the 50% inhibitory concentration (IC_{50}) was determined to be 6 nM and 25 nM for the lac-PEGylated polyplex and ace-PEGylated polyplex, respectively (Figure 5). This almost fourfold increase in the growth-inhibitory effect exerted by lac-PEGylated polyplex is likely to be due to the facilitated uptake into the HuH-7 cells through an ASGP receptor-mediated endocytosis process.[5] This long-term growth-inhibitory effect (up to 21 days) on the spheroids by the single dose of PEGylated polyplexes added at the beginning is worth noting. The control lac-PEGylated polyplex, which included a siRNA against the firefly luciferase sequence (Luc-lac-PEGylated polyplex), induced almost no growth-inhibitory effect even at a conjugate concentration of 100 nM, strongly suggesting that the observed growth-inhibitory effect of the PEGylated polyplexes on the HuH-7 spheroids indeed occurred in a sequence-specific manner (Figure 3 and 4). Although the lipoplexes showed a higher growth-inhibitory effect than the PEGylated polyplex system on monolayer-cultured HuH-7 cells (Figure 2), almost no growth-inhibitory effect on the HuH-7 spheroids was observed even at a siRNA concentration of 100 nM (Figures 3 and 4a). This is presumably due to the cationic nature of the lipoplexes interacting nonspecifically with the negatively charged cell membrane and ECM, which leads to poor penetration into the HuH-7 spheroids. In addition, the spheroid size did not influence the growth-inhibitory effect of the PEGylated polyplexes; the lac-PEGylated polyplexes showed a significant growth-inhibitory effect on the HuH-7 spheroids with an initial diameter of both 200 (data not shown) and 250 μm (Figure 3), whereas the lipoplexes showed almost no growth-inhibitory effect even at high siRNA concentrations (100 nM).

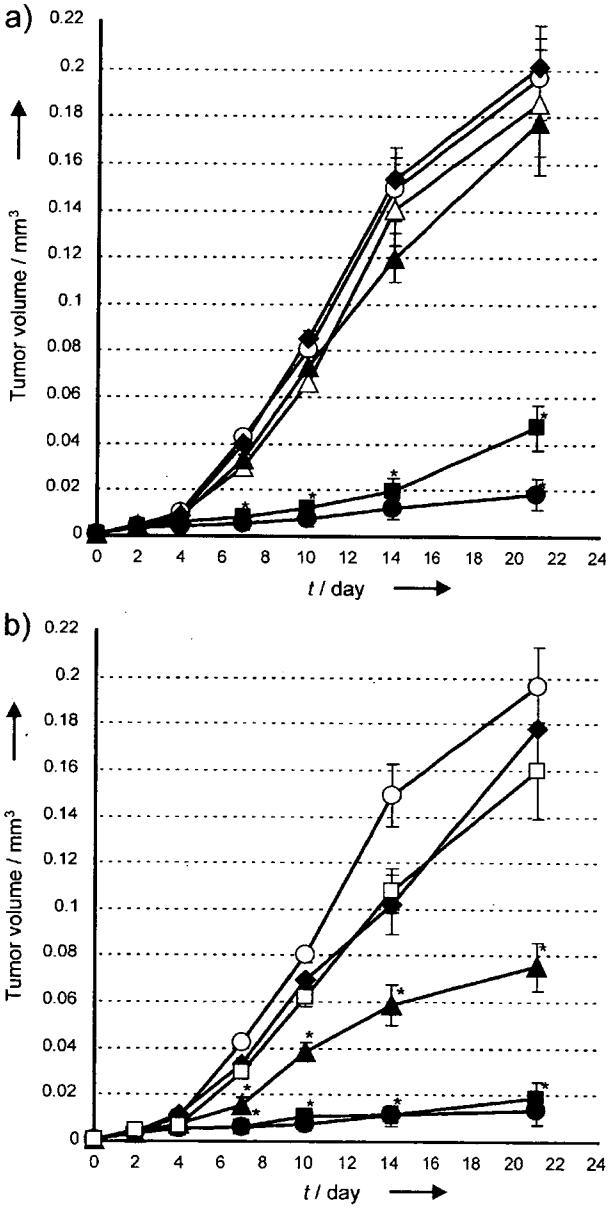

Figure 4. Time-dependent change in the volume of the spheroids treated with a) ace-PEGylated polyplexes and b) lac-PEGylated polyplexes; mock (open circles), OligofectAMINE at [siRNA] = 100 nM (open triangles), Luc-lac-PEGylated polyplex at [conjugate] = 100 nM (open squares), and the PEGylated polyplexes at [conjugate] = 100 nM (closed circles), 50 nM (closed squares), 10 nM (closed triangles), and 1 nM (closed lozenges). The volume of the spheroids was calculated as described in the Experimental Section. The data are averages of five HuH-7 spheroids ±SD. The data points marked with asterisks are statistically significant compared with the mock data (buffer-treated cells) ($P^* < 0.05$).

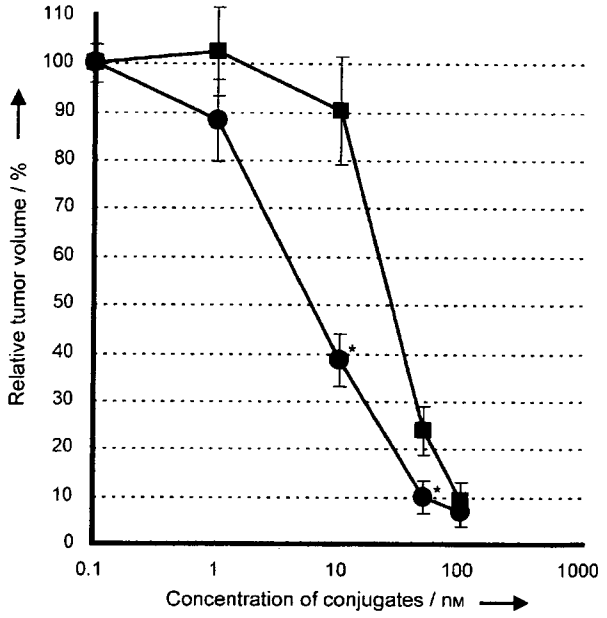

Figure 5. Effect of the complexed PEG-siRNA conjugate concentration on the growth inhibition of the HuH-7 spheroids with an initial diameter of 100 μm (closed squares: ace-PEGylated polyplexes; closed circles: lac-PEGylated polyplexes). The relative spheroid volume as the vertical axis was defined as the ratio of volume of the HuH-7 spheroids treated with PEGylated polyplexes to that of the mock sample on day 21. The data are averages of five HuH-7 spheroids ±SD. The data points for the lac-PEGylated polyplexes marked with asterisks are statistically significant compared with those for the ace-PEGylated polyplexes at the corresponding concentrations ($P^* < 0.05$).

Effect of the PLL length on the growth inhibition of spheroids by the PEGylated polyplexes

The effect of the PLL length on the growth inhibition of spheroids induced by the lac-PEGylated polyplexes was then examined. PLLs with varying DPs (40, 100, or 460) were used to prepare the PEGylated polyplex of the PEG-siRNA conjugate. As can be seen in Figure 6a, a striking effect of the PLL length on the growth inhibition of HuH-7 spheroids was observed at a conjugate concentration of 10 nM; the lac-PEGylated polyplexes prepared from shorter PLL (DP = 40) showed only limited efficacy relative to those from longer PLLs (DP = 100 or 460). Consequently, the IC_{50} was determined to be 7 nM, 6 nM, and 70 nM for the lac-PEGylated polyplexes prepared from PLL with DP = 460, DP = 100, and DP = 40, respectively (Figure 6b). These results indicate that the lac-PEGylated polyplexes formed from shorter PLL (DP = 40) are probably unstable under the extremely dilute conditions because of the critical dissociation phenomenon,[16] resulting in the impaired cellular uptake of the Lac-PEG-siRNA conjugate.

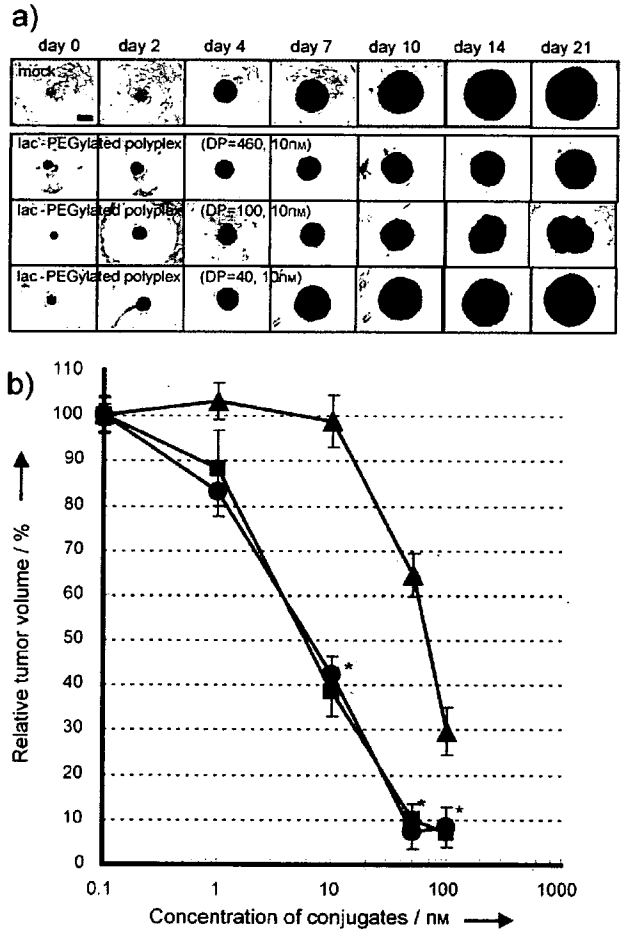

Figure 6. Effect of the PLL length on the growth-inhibitory effect of the lac-PEGylated polyplexes on the HuH-7 spheroids with an initial diameter of 100 μm (bar = 100 μm). a) Phase-contrast images of spheroids treated with the lac-PEGylated polyplexes composed of PLL with varying chain lengths. b) Change in the relative volume of the HuH-7 spheroids on day 21 with various concentrations of lac-PEGylated polyplexes composed of PLL with varying chain lengths (closed triangles: DP = 40; closed squares: DP = 100; closed circles: DP = 460). The relative spheroid volume as the vertical axis was defined as the ratio of volume of the HuH-7 spheroids treated with PEGylated polyplexes to that of the mock sample on day 21. The data are averages of five HuH-7 spheroids ± SD. The data points marked with asterisks are statistically significant compared with those for the lac-PEGylated polyplexes (DP = 40) at the corresponding concentrations ($P^* < 0.05$).

Distribution of the PEGylated polyplexes in multicellular tumor spheroids

To confirm whether or not the lac-PEGylated polyplex can effectively penetrate into the HuH-7 spheroids, 5'-FITC-labeled (fluorescein isothiocyanate) oligodeoxynucleotide (ODN) having the same antisense sequence as the firefly luciferase siRNA was hybridized with the sense firefly luciferase PEG-ODN conjugate to form an FITC-labeled Lac-PEG-dsODN conjugate. The FITC-labeled conjugate was mixed with PLL (DP = 100) at an N/P ratio of 1 to form a PEGylated polyplex with the FITC-label (FITC-PEGylated polyplex). An FITC-labeled lipoplex was also prepared by mixing the OligofectAMINE with FITC-labeled dsODN having the same sequence as the firefly luciferase siRNA. The fluorescence of the FITC-labeled lipoplexes and the FITC-PEGylated polyplexes was observed under a confocal fluorescence-scanning microscope after 48 h of incubation as shown in Figure 7. Most of the fluorescence from the FITC-labeled lipoplexes was seen only at the periphery of the HuH-7 spheroid even after 48 h of incubation (Figure 7a), indicating that the lipoplexes have a poor ability to penetrate into the HuH-7 spheroids, presumably due to the large complex size and the strong interaction with the negatively charged cell membrane and/or ECM.[17] This poor penetration of the lipoplexes into the HuH-7 spheroids obviously has a negative effect on the RecQL1 siRNA-mediated growth inhibition. In sharp contrast, the fluorescence from the FITC-PEGylated polyplexes was observed not only at the periphery but also much

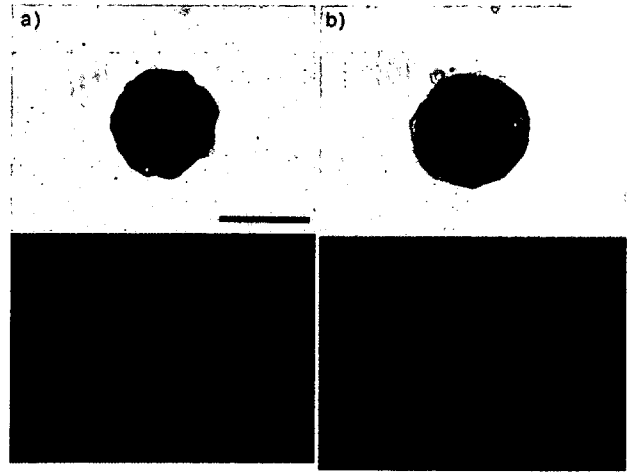

Figure 7. Distribution in the HuH-7 spheroids of the a) FITC-labeled dsODN in the OligofectAMINE lipoplexes (z-axis: 87 μm) and b) FITC-labeled Lac-PEG-dsODN conjugate in the lac-PEGylated polyplexes (z-axis: 79 μm) after 48 h of incubation. Initial diameter of the spheroids: 100 μm (bar = 200 μm).

farther in the interior of the HuH-7 spheroids (Figure 7b) than that of the FITC-labeled lipoplexes after 48 h of incubation (Figure 7b). This result suggests that the small size of approximately 100 nm and the nonionic and hydrophilic PEG shell of the PEGylated polyplexes may reduce the nonspecific interaction of the micelles with the cell membrane and/or ECM, allowing their smooth penetration into the HuH-7 spheroids.[18]

Detection of apoptosis in the HuH-7 spheroids

To confirm whether or not the observed growth-inhibitory effect of the PEGylated polyplexes on the HuH-7 spheroids is due to the induction of cell death, a Live/Dead staining assay was carried out for the HuH-7 spheroids treated with mock, lipoplex (100 nM), and lac-PEGylated polyplex (50 nM), respectively. By means of confocal fluorescence-scanning microscopy, living and dead cells in the HuH-7 spheroids were individually detected as green fluorescence and red fluorescence, respectively. As can be seen in Figure 8, cell death at the center of the mock-treated HuH-7 spheroid was clearly observed on day 7, whereas living cells were only observed at the periphery of the spheroid. The observed cell death in the mock-treated sample was apparently due to necrosis resulting from the insufficient supply of oxygen and nutriment to the spheroid interior, deficiencies which become significant with increasing spheroid size.[11] Note that the spheroids treated with the lipoplexes showed some zones at the periphery containing dead cells on day two, yet after ten days the distribution of dead and living cells was the same as in the mock-treated samples. In contrast, the spheroids treated with lac-PEGylated polyplexes showed continuous cell death at the periphery even after day ten, resulting in the significant death of cells in the spheroids.

In addition to the Live/Dead staining assay, we performed the detection of activated caspase-3 in the HuH-7 spheroids to confirm the induction of apoptosis. The activation of caspase-3 is known to play a central role in the induction of the apoptosis;[19] therefore, caspase-3 is an appropriate marker for measuring apoptosis induced by RecQL1 siRNA. Activated caspase-3 was detected using Magic Red fluorescence probe (MR-$(DEVD)_2$). In the presence of activated caspase-3, the DEVD amino-acid sequence in the MR-$(DEVD)_2$ is cleaved to generate a red fluorescence.[20] As can be seen in Figure 9, apoptotic cells (fluorescence signals) were not observed in the mock-treated spheroids. In contrast, apoptotic cells (fluorescent signals) were observed at the periphery of the spheroids treated with the lipoplex as early as day one. Nevertheless, there was no sign of apoptosis after seven days. It is worth noting that the apoptotic cells were also observed at the periphery of spheroids treated with the lac-PEGylated polyplex, and the number of apoptotic cells increased with prolonged incubation time, from day four to day ten. Note that apoptotic cells were still observed even after ten days. Other spheroids treated with the lac-PEGylated polyplex also showed a similar tendency. These results strongly suggest that the observed growth-inhibitory effect and cell death in the spheroids treated with PEGylated polyplexes are likely to be due to apoptosis induced by RecQL1 siRNA in the long term. In addition, the significant difference in the observation period for apoptotic cells between the PEGylated polyplexes and the lipoplexes may be ascribed to the lower tolerance of the lipoplexes for the culture environment than the PEGylated polyplexes. The appreciable stability under physiological conditions and the uniform size of 100 nm of the PEGylated polyplexes may contribute to their smooth penetration into the spheroids, eventually facilitating the RNAi effect through the continuous uptake into the tumor cells located in the interior and the periphery of the spheroids.

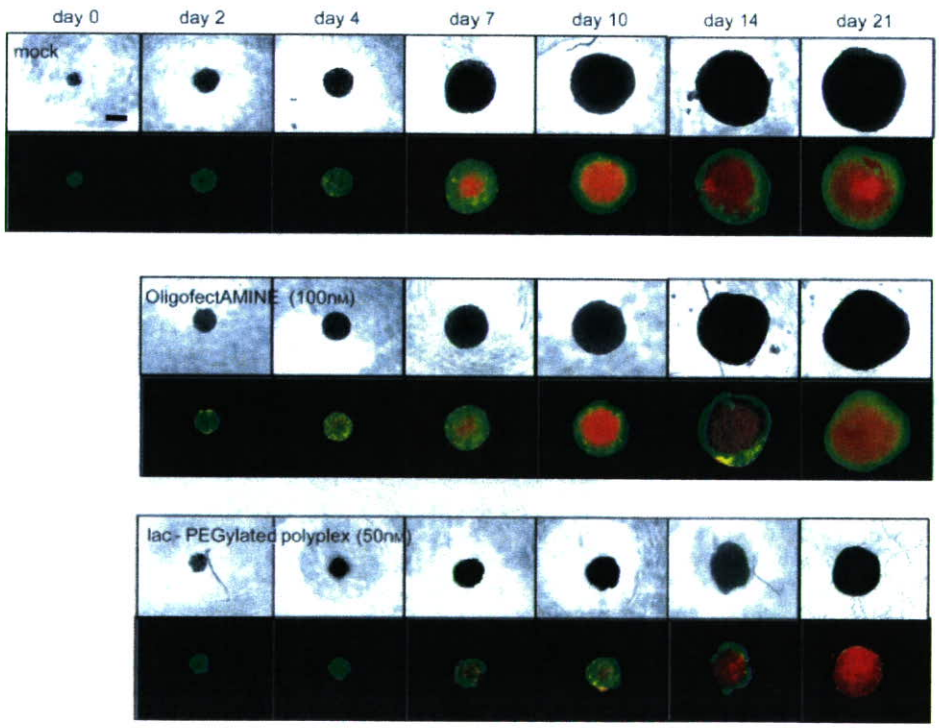

Figure 8. Live/Dead staining assay of the HuH-7 spheroids treated with mock, OligofectAMINE ([siRNA] = 100 nM) and lac-PEGylated polyplexes ([conjugate] = 50 nM) (bar = 100 μm). Living and dead cells emit green and red fluorescences, respectively.

Conclusions

In conclusion, we have demonstrated that MCTSs are useful for evaluating the long-term (up to 21 days) efficacy of siRNA delivery systems (therapeutic value). Note that MCTSs are a versatile in vitro model which can be

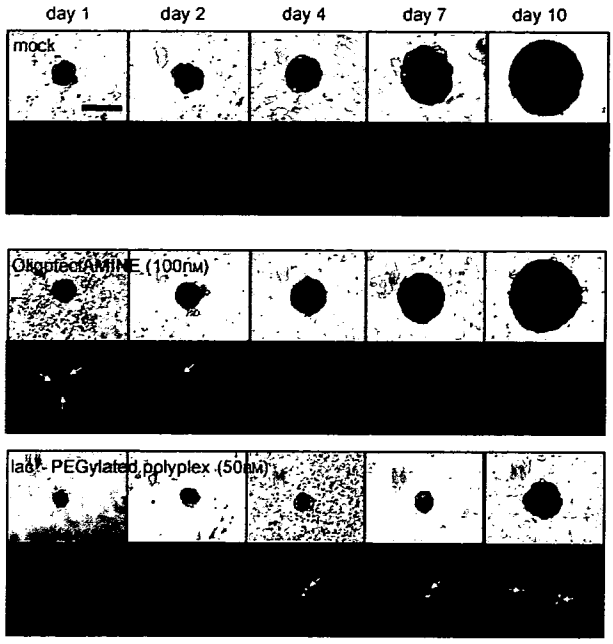

Figure 9. Detection of the activated caspapase-3 as the signal of apoptosis in the HuH-7 spheroids treated with mock, OligofectAMINE ([siRNA] = 100 nM), and lac-PEGylated polyplexes ([conjugate] = 50 nM) (bar = 200 μm).

used to estimate the penetration of carriers into 3D tumor tissues and the effect of the ECM and cell-cell contacts (microenvironment) that could otherwise only be examined in vivo using animal models. Indeed, the lac-PEGylated polyplexes composed of the Lac-PEG-siRNA conjugate and PLL showed a remarkable growth-inhibitory effect (IC_{50} = 6 nM) on the HuH-7 spheroids, inducing long-term apoptotic cell death by means of RecQL1 siRNA. Several important factors are likely to be synergistically involved in the pronounced growth-inhibitory effect of the PEGylated polyplexes, such as the improvement of the stability against enzymatic degradation, smooth penetration into the spheroid interior, and enhancement of the cellular uptake through ASGP receptor-mediated endocytosis. In sharp contrast, the lipoplexes showed almost no growth-inhibitory effect even at a siRNA concentration 100 nM in the HuH-7 spheroids, presumably due to the poor penetration into the spheroids. Furthermore, spheroids derived directly from patients' tumor tissues offer the opportunity of studying the efficacy of delivery systems in the unique tumor cell microenvironments characteristic to individual patients. Thus, MCTSs, as an in vitro tumor model, are expected to be useful in the assessment of the usefulness of siRNA carrier systems in tumor targeting.

Experimental Section

Materials: PLLs (degree of polymerization (DP) = 40, M_w = 8300; DP = 100, M_w = 20900; DP = 460, M_w = 75900) were purchased from Sigma. OligofectAMINE and LipofectAMINE were purchased from Invitrogen. 5'-Thiol-modified sense RNAs (HS-$(CH_2)_6$-CUU ACG CUG AGU ACU UCG AdTdT-3', firefly luciferase, pGL3-control sense sequence[1] and HS-$(CH_2)_6$-GUU CAG ACC ACU UCA GCU UdTdT-3', RecQL1, sense sequence[10]) and unmodified antisense RNA (5'-UCG AAG UAC UCA GCG UAA GdTdT-3', firefly luciferase, pGL3-control antisense sequence and 5'- AAG CUG AAG UGG UCU GAA CdTdT-3', RecQL1, antisense sequence) were purchased from Dharmacon. Water was purified using a Milli-Q instrument (MILLIPORE). Plasmid DNAs (pDNA) encoding firefly luciferase (pGL3-Control, Promega; 5256 bp) and renilla luciferase (pRL-TK, Promega; 4045 bp) were amplified using EndoFree Plasmid Maxi or Mega Kits (QIAGEN). The DNA concentration was determined by reading the absorbance at 260 nm. A spheroid culture plate, Celltight Spheroid Culture Plate, was purchased from Sumitomo Bakelite. MTT assay reagents and a double staining kit (Live/Dead assay) were purchased from DOJINDO. A Magic Red Caspase Detection Kit was purchased from Immunochemistry Technologies.

Preparation of the PEGylated polyplexes: The PEG-siRNA conjugates were prepared as described in the previous report.[5] Specific amounts of the PEG-siRNA conjugate (50 μM) and PLL were separately added to 10 mM Tris-HCl buffer (pH 7.4) to prepare the 10 μM stock solutions. The solutions were filtered through a 0.1 μm filter to remove the dust. The PEG-siRNA conjugate in 10 mM Tris-HCl buffer (pH 7.4) was mixed with PLL stock solution in 10 mM Tris-HCl buffer (pH 7.4) at an equal unit molar ratio of phosphate groups in the PEG-siRNA conjugate to amino groups in PLL (N/P = 1), followed by the addition of 10 mM Tris-HCl buffer (pH 7.4), adding 0.3 M NaCl to adjust the ionic strength of the solution to the physiological condition (0.15 M NaCl).

Cell culture: HuH-7 human cancer cells, derived from a hepatocarcinoma cell line, were obtained from the Cell Resource Center for Biomedical Research, Institute of Development, Aging, and Cancer, Tohoku University. The monolayer-cultured cells and multicellular spheroids were grown in Dulbecco's modified Eagle's medium (DMEM) supplemented with 10% FBS, 100 units/mL penicillin, and 100 μg mL^{-1} streptomycin at 37°C in a humidified 5% CO_2 atmosphere.

MTT assay: HuH-7 cells were plated in a 96-well plate (10^4 cells/well) to allow them to reach about 50% confluence after 24 h and the medium was then changed to fresh DMEM with 10% FBS (180 μL/well). To each well, appropriate amounts of sample were added in 20 μL aliquot. After 48 h of incubation, fresh medium (100 μL/well) was added, and further incubation was carried out for 48 h. The metabolic activity of each well was determined by an MTT assay. The optical absorbance was measured at 560 nm using a microplate reader and converted to the percentage relative to that for mock cells (buffer-treated cells).

Growth inhibition of the HuH-7 spheroids: Single-cell suspensions were obtained by the trypsinization of monolayer-cultured HuH-7 cells: 45 μL of single-cell suspensions (80 cells) were seeded in individual wells of a 96-well Celltight Spheroid Culture Plate to form the 100 μm HuH-7 spheroids. After 24 h, the PEGylated polyplexes (N/P = 1), siRNA, Lac-PEG-siRNA conjugate or OligofectAMINE/siRNA (5 μL/well) were added to the well at the prescribed concentration on day 0. Fresh DMEM with 10% FBS was added to each wells on day 2 (25 μL/well), 7 (50 μL/well), 10 (50 μL/well), and 14 (50 μL/well), compensating for the decrease in the medium volume due to the natural evaporation. The perpendicular diameters of the HuH-7 spheroids were measured by means of phase-contrast microscope (Olympus IX71) on day 0, 2, 4, 7, 10, 14, and 21. The volume of the HuH-7 spheroids was calculated using the following formula:[21]

$$4\pi a^2 b/3 = \text{Tumor Volume (mm}^3\text{)}, \quad (1)$$

where *a* and *b* are the smallest and largest radius (mm) of the HuH-7 spheroids, respectively.

Distribution study of FITC-labeled oligodeoxynucleotide in the HuH-7 spheroids: 5'-FITC-labeled (fluorescein isothiocyanate) oligodeoxynucleotide (ODN) having the same antisense sequence as the firefly luciferase siRNA was hybridized with the sense firefly luciferase PEG-ODN conjugate to form an FITC-labeled Lac-PEG-dsODN conjugate. The lac-PEGylated polyplex was then prepared by mixing FITC-labeled Lac-PEG-dsODN conjugate with PLL (DP = 100). FITC-labeled dsDNA/OligofectAMINE was also prepared as the control. FITC-PEGylated polyplexes or FITC-dsODN/OligofectAMINE were added to the 100 μm HuH-7 spheroids at conjugate or siRNA concentration of 400 nM, and incubated for 48 h. After the incubation, the HuH-7 spheroids were washed three times with phosphate-buffered saline (PBS) and imaged directly in the cell culture medium using a confocal fluorescence-scanning microscope (Olympus IX71 equipped with a confocal IX2-DSU system and an appropriate filter).

Live/Dead staining assay: A Live/Dead staining assay was carried out using a double staining kit. The staining solution (15 μL) containing calcein-acetoxymethyl (10 μM) and propidium iodide (30 μM) were added to the HuH-7 spheroids (100 μm initial diameter) treated with the lac-PEGylated polyplexes (50 nM), OligofectAMINE/siRNA (100 nM), or mock on day 0, 2, 4, 7, 10, 14, and 21. After 2 h of incubation, the HuH-7 spheroids were washed three times with PBS and imaged directly in the cell culture medium using a confocal fluorescence-scanning microscope (Olympus IX71 equipped with a confocal IX2-DSU system and an appropriate filter).

Detection of apoptosis: The detection of apoptosis was carried out using a Magic Red Caspase Detection Kit. Staining solution (5 μL) containing MR-$(DEVD)_2$ (30 μM) were added to the HuH-7 spheroids (100 μm initial diameter) treated with the lac-PEGylated polyplexes (50 nM), OligofectAMINE/siRNA (100 nM) or mock on day 0, 1, 2, 4, 7, 10, 14, and 21. After 2 h of incubation, the HuH-7 spheroids were washed three times with PBS and imaged directly in the cell culture medium using a confocal fluorescence-scanning microscope (Olympus IX71 equipped with a confocal IX2-DSU system and an appropriate filter).

Acknowledgements

This study was partially supported by the Core Research for Evolutional Science and Technology (CREST) program of the Japan Science and Technology Agency (JST) and by the Cell Science Research Foundation.

Keywords: antitumor agents · bioconjugates · drug delivery · siRNA · spheroids

[1] S. M. Elbashir, J. Harborth, W. Lendeckel, A. Yalcin, K. Weber, T. Tuschl, *Nature* **2001**, *411*, 494.
[2] A. Fire, S. Xu, M. K. Montgomery, S. A. Kostas, S. E. Driver, C. C. Mello, *Nature* **1998**, *391*, 806.
[3] D. A. Braasch, Z. Paroo, A. Constantiescu, G. Ren, O. K. Oz, R. P. Mason, D. R. Corey, *Bioorg. Med. Chem. Lett.* **2004**, *14*, 1139.
[4] a) R. M. Schiffelers, A. Ansari, J. Xu, Q. Zhou, Q. Tang, G. Storm, G. Molema, P. Y. Lu, P. V. Scaria, M. C. Woodle, *Nucleic Acids Res.* **2004**, *32*, e149; b) J. Yano, K. Hirabayashi, S. Nakagawa, T. Yamaguchi, M. Nogowa, I. Kashimori, H. Naito, H. Kitagawa, K. Ishiyama, T. Ohgi, T. Irimura, *Clin. Cancer Res.* **2004**, *10*, 7721; c) C. N. Landen, Jr., A. Chavez-Reyes, C. Bucana, R. Schmandt, M. T. Deavers, G. Lopez-Berestein, A. K. Sood, *Cancer Res.* **2005**, *65*, 6910; d) S. Hu-Lieskovan, J. D. Heidel, D. W. Bartlett, M. E. Davis, T. J. Triche, *Cancer Res.* **2005**, *65*, 8984.
[5] M. Oishi, Y. Nagasaki, K. Itaka, N. Nishiyama, K. Kataoka, *J. Am. Chem. Soc.* **2005**, *127*, 1624.
[6] Y. Furuichi, *Ann. N. Y. Acad. Sci.* **2000**, *928*, 121.
[7] a) K. M. Doherty; S. Sharma, L. A. Uzdilla, T. M. Wilson, S. Cui, A. Vindigni, R. M. Brosh, Jr., *J. Biol. Chem.* **2005**, *280*, 28085; S. Sharma, L. A. Uzdilla, T. M. Wilson, S. Cui, A. Vindigni, R. M. Brosh, Jr., *J. Biol. Chem.* **2005**, *280*, 28085; b) S. Sharma, J. A. Sommers, S. Choudhary, J. K. Faulkner, S. Cui, L. Andreoli, L. Muzzolini, A. Vindigni, R. M. Brosh, Jr., *J. Biol. Chem.* **2005**, *280*, 28072.
[8] G. LeRoy, R. Carroll, S. Kyin, M. Seki, M. D. Cole, *Nucleic Acids Res.* **2005**, *33*, 6251.
[9] T. Kawabe, N. Tsuyama, S. Kitao K. Nishikawa, A. Shimamoto, M. Shiratori, T. Matsumoto, K. Anno, T. Sato, Y. Mitsui, M. Seki, T. Enomoto, M. Goto, N. A. Ellis, T. Ide, Y. Furuichi, M. Sugimoto, *Oncogene* **2000**, *19*, 4764.
[10] M. Takagi, A. Shimamoto, Y. Furuichi, A. Sato, WO/2004100990, **2004**.
[11] a) A. Moscona, *Proc. Natl. Acad. Sci. USA* **1957**, *43*, 184; b) R. M. Sutherland, *Science* **1988**, *240*, 177; c) M. T. Santini, G. Rainaldi, P. L. Indovina, *Int. J. Radiat. Biol.* **1999**, *75*, 787.
[12] G. Y. Wu, C. H. Wu, *Adv. Drug Delivery Rev.* **1998**, *29*, 243.
[13] a) J. E. Moulder, S. Rockwell, *Cancer Metastasis Rev.* **1987**, *5*, 313; b) A. L. Harris, *Nat. Rev. Cancer* **2002**, *2*, 38; c) M. Dean, T. Fojo, S. Bates, *Nat. Rev. Cancer* **2005**, *5*, 275.
[14] H. R. Mellor, L. A. Davies, H. Caspar, C. R. Pringle, S. C. Hyde, D. R. Gill, R. Callaghan, *J. Gene Ther.* **2006**, *8*, 1160.
[15] M. A. Konerding, E. Fait, A. Gaumann, *Br. J. Cancer* **2001**, *84*, 1354.
[16] M. Oishi, F. Nagastugi, S. Sasaki, Y. Nagasaki, K. Kataoka, *ChemBioChem* **2005**, *6*, 718.
[17] R. Parthasarathy, P. G. Sscks, D. Harris, H. Brock, K. Mehta, *Cancer Chemother. Pharmacol.* **1994**, *34*, 527.
[18] Y. Bae, N. Nishiyama, S. Fukushima, H. Koyama, Y. Matsumura, K. Kataoka, *Bioconjugate Chem.* **2005**, *16*, 122.
[19] N. A. Thornberry, *Chem. Biol.* **1998**, *5*, R97.
[20] N. A. Thornberry, T. A. Rano, E. P. Peterson, D. M. Rasper, T. Timkey, M. Gracia-Calvo, V. M. Houtzager, P. A. Nordstrom, S. Roy, J. P. Vaillancourt, K. T. Chapman, D. W. Nicholson, *J. Biol. Chem.* **1997**, *272*, 17907.
[21] T. Fujiwara, E. A. Grimm, T. Mukhopadhyay, D. W. Cai, L. B. Owen-Schaub, J. A. Roth, *Cancer Res.* **1993**, *53*, 4129.

Received: April 2, 2007
Revised: April 30, 2007
Published online on June 4, 2007

Dendrimer Generation Effects on Photodynamic Efficacy of Dendrimer Porphyrins and Dendrimer-Loaded Supramolecular Nanocarriers

Yuan Li,[†] Woo-Dong Jang,*[,‡] Nobuhiro Nishiyama,[§] Akihiro Kishimura,[†,+,@] Satoko Kawauchi,[∥] Yuji Morimoto,[∥] Sayaka Miake,[⊥] Takashi Yamashita,[⊥] Makoto Kikuchi,[∥] Takuzo Aida,[#,@] and Kazunori Kataoka*[,†,§,+,@]

Department of Materials Engineering, Graduate School of Engineering, The University of Tokyo, 7-3-1 Hongo, Bunkyo-ku, Tokyo 113-8656, Japan, Department of Chemistry, College of Science, Yonsei University, 134 Sinchondong, Seodaemun-gu, Seoul 120-749, Korea, Center for Disease Biology and Integrative Medicine, Graduate School of Medicine, The University of Tokyo, 7-3-1 Hongo, Bunkyo-ku, Tokyo 113-0033, Japan, Department of Medical Engineering, National Defense Medical College, 3-2 Namiki, Tokorozawa, Saitama 359-8513, Japan, Department of Pure and Applied Chemistry, Faculty of Science and Technology, Tokyo University of Science, 2641 Yamazaki, Noda-shi, Chiba 278-8510, Japan, Department of Chemistry and Biotechnology, Graduate School of Engineering, The University of Tokyo, 7-3-1 Hongo, Bunkyo-ku, Tokyo 113-8656, Japan, Core Research for Evolutional Science and Technology (CREST), Japan Science and Technology Agency (JST), and Center for NanoBio Integration, The University of Tokyo, 7-3-1 Hongo, Bunkyo-ku, Tokyo 113-8656, Japan

Received May 29, 2007. Revised Manuscript Received July 17, 2007

A series of poly(benzyl ether) dendrimer porphyrins (DPs) (Gn = n-generation dendrimer, n = 1−3) was examined as potential photosensitizers for photodynamic therapy (PDT). Polyion complexes (PICs) between the DPs and poly(ethylene glycol)-*block*-poly(L-lysine) (PEG-*b*-PLL) were formed via an electrostatic interaction between the positively charged poly(L-lysine) (PLL) segment and negatively charged periphery of the DPs. Dynamic light scattering (DLS) measurements and transmission electron microscopy (TEM) showed that G3 formed a core−shell-type nanocarrier micelle, whereas G1 and G2 formed irregular-shaped nanoparticles with a relatively high polydispersity. The photophysical properties of the DP-loaded PIC nanocarriers strongly depend on the generation of the DPs. In the case of G1 and G2, their fluorescence lifetime and oxygen consumption ability were significantly reduced by the formation of the PIC nanocarriers, whereas the G3-loaded PIC nanocarrier exhibited almost comparable fluorescence lifetimes and oxygen consumption abilities to the free G3. The incorporation of DPs into PIC nanocarriers resulted in an appreciable increase in the cellular uptake, yet inversely correlated with the generation. Alternatively, the photocytotoxicity of the DPs within the nanocarriers increased with an increase in the generation despite a decrease in the cellular uptake. By correlating the effects of the uptake amount with the photocytotoxicity, the PIC nanocarriers showed remarkable enhancement of the PDT efficacy dependent on the generation of DPs.

Introduction

Dendrimers with predictable three-dimensional architectures are currently undergoing fast growth in various applications. This is due in part to the variety of applications being pursued for dendrimers.[1,2] In particular, application of dendrimers to biomedical uses has attracted much attention due to the tunable properties of the dendrimer generation, terminal groups, and inner cavity for the incorporation of a variety of molecules.[1−6] PAMAM dendrimers, for example, have been comprehensively investigated as diagnostic tools and drug carriers.[6−8] Recently, we have reported the third generation poly(benzyl ether) dendrimer porphyrins (DPs) as an effective photosensitizer for photodynamic therapy (PDT).[9−11]

PDT involves the administration of a photosensitizer, which preferentially accumulates in target tissues. Subsequent

* To whom correspondence should be addressed. Phone: +81-3-5841-7138. Fax: +81-3-5841-7139. E-mail: kataoka@bmw.t.u-tokyo.ac.jp.
† Department of Materials Engineering, The University of Tokyo.
‡ Yonsei University.
§ Center for Disease Biology and Integrative Medicine, The University of Tokyo.
∥ National Defense Medical College.
⊥ Tokyo University of Science.
Department of Chemistry and Biotechnology, The University of Tokyo.
+ CREST.
@ Center for NanoBio Integration, The University of Tokyo.

(1) *Dendrimers and other Dendritic Polymers*; Fréchet, J. M. J., Tomalia, D. A., Eds.; John Wiley & Sons: New York, 2001.
(2) Bosman, A. W.; Janssen, H. M.; Meijer, E. W. *Chem. Rev.* **1999**, *99*, 1665−1688.
(3) Lee, I.; Athey, B. D.; Wetzel, A. W.; Meixner, W.; Baker, J. R., Jr. *Macromolecules* **2002**, *35*, 4510−4520.
(4) Roy, R.; Zanini, D.; Meunier, S. J.; Romanowska, A. *J. Chem. Soc., Chem. Commun.* **1993**, 1869−1872.
(5) Jang, W.-D.; Kataoka, K. *J. Drug Delivery Sci. Technol.* **2005**, *15*, 19−30.
(6) Wiener, E. C.; Brechbiel, M. W.; Brothers, H.; Magin, R. L.; Gansow, O. A.; Tomalia, D. A.; Lauterbur, P. C. *Magn. Reson. Med.* **1994**, *31*, 1−8.
(7) Malik, N.; Evagorou, E. G.; Duncan, R. *Anti-Cancer Drugs* **1999**, *10*, 767−776.
(8) Maruyama-Tabata, H.; Harada, Y.; Matsumura, T.; Satoh, E.; Cui, F.; Iwai, M.; Kita, M.; Hibi, S.; Imanishi, J.; Sawada, T.; Mazda, O. *Gene Ther.* **2000**, *7*, 53−60.

10.1021/cm071451m CCC: $37.00
Published on Web 10/11/2007